

Challenge Journal of **CONCRETE RESEARCH LETTERS**

Vol.10 No.2 (2019)

CFRP acidic environment acoustic emission
compressive strength concrete
corrosion cracking curing ductility
durability energy absorption ferrocement
flaky aggregate fly ash fracture mortar
palm oil fuel ash reinforced concrete
self-compacting concrete silica fume steel
fibers strength superplasticizer water
absorption water-cement ratio workability



TULPAR
ACADEMIC PUBLISHING

ISSN 2548-0928



Challenge Journal

OF CONCRETE RESEARCH LETTERS

EDITOR IN CHIEF

Prof. Dr. Mohamed Abdelkader ISMAIL

Miami College of Henan University, China

EDITORIAL BOARD

Prof. Dr. Abdullah SAAND	<i>Quaid-e-Awam University of Engineering, Pakistan</i>
Prof. Dr. Alexander-Dimitrios George TSONOS	<i>Aristotle University of Thessaloniki, Greece</i>
Prof. Dr. Ashraf Ragab MOHAMED	<i>Alexandria University, Egypt</i>
Prof. Dr. Ayman NASSIF	<i>University of Portsmouth, United Kingdom</i>
Prof. Dr. Gamal Elsayed ABDELAZIZ	<i>Benha University, Egypt</i>
Prof. Dr. Han Seung LEE	<i>Hanyang University, Republic of Korea</i>
Prof. Dr. Zubair AHMED	<i>Mehran University, Pakistan</i>
Prof. Dr. Jiwei CAI	<i>Henan University, China</i>
Dr. Aamer Rafique BHUTTA	<i>Universiti Teknologi Malaysia, Malaysia</i>
Dr. Khairunisa MUTHUSAMY	<i>Universiti Malaysia Pahang, Malaysia</i>
Dr. Mahmoud SAYED AHMED	<i>Ryerson University, Canada</i>
Dr. Jitendra Kumar SINGH	<i>Hanyang University, Republic of Korea</i>
Dr. Meral OLTULU	<i>Atatürk University, Turkey</i>
Dr. Saleh Omar BAMAGA	<i>University of Bisha, Saudi Arabia</i>

E-mail: cjcr@challengejournal.com

Web page: cjcr.challengejournal.com

TULPAR Academic Publishing
www.tulparpublishing.com





CONTENTS

Research Articles

Composite concrete beam with multi-web cold-formed steel section 20-33

Ahmed Youssef Kamal, Nader Nabih Khalil

Properties of self-compacting concrete containing granite dust particles 34-41

Joseph Abah Apeh

Effect of nano silica on cement mortars containing micro silica 42-49

İlknur Bekem Kara, Ömer Furkan Durmuş



Research Article

Composite concrete beam with multi-web cold-formed steel section

Ahmed Youssef Kamal * , Nader Nabih Khalil 

Department of Civil Engineering, Benha University, Benha, Egypt

ABSTRACT

Lately, structural engineers use cold-formed steel sections (CFS) in buildings due to its light-weight and easy shaping. Encasing the cold-formed steel sections by concrete avoiding the structure elements some of its disadvantages especially buckling. This paper reports an experimental test program for beams with a multi-web cold-formed steel section encased by reinforced concrete. Eleven (full-scale) specimens have tested under mid-span concentrated load, the experimental test program designed to cover many cold-formed steel section variables such as (web number, web height, and the steel section length). Comparison between the experimental results for specimens with encased steel cold-formed section and that for reference beam have presented. The experimental results show that the cold-formed steel webs number has a noticeable influence on the structural behaviour of the beam, such as increasing the beam load capacity. The beam load capacity, failure mode and the beam ductility have analysed, and some preparatory criteria for a sufficient outline have presented.

ARTICLE INFO

Article history:

Received 19 August 2018

Revised 2 February 2019

Accepted 30 April 2019

Keywords:

Composite concrete beam

Encased

Multi-web

Cold-formed steel

CFS

1. Introduction

Cold-formed steel members have broadly used as a part of the structural building because of their high strength-weight ratio, and for their ease and low-cost of manufacture. Yu (2010) has summarized the commonly used cold-formed steel section shapes for different applications. United States manufacturing associations introduced catalogs for the cold-formed steel (CFS) shapes, such as that provided by the Steel Framing Industry Association (SFIA) (2012). Cold forming technology restricts the cold-formed steel members' thickness in a range between 0.8 and 3 mm, Hancock (2007).

The buckling of the element cross-section under compression or shear may occur before the overall member failure; this phenomenon called local buckling. Thus, the CFS local buckling becomes a hindrance to the extensive use of thin-walled sections. Modifying the CFS cross-sections shape can significantly enhance the structure member load capacity and overcome the problem of local buckling in addition to reducing costs compared to the commonly used shapes "U-section, C-section, etc." However, previous researchers, focused on solutions

leading to cross-sections that cannot be effectively manufactured by the current cold-forming processes (Gilbert et al., 2012a, 2012b; Wang et al., 2016; Liu et al., 2004; Madeira et al., 2015; Leng et al., 2011; Moharrami et al., 2014). Pham et al. (2014) have reported that providing a longitudinal web stiffener in the direction of the longitudinal stresses reduces the web local buckling. Ye et al. (2016) said that, adding intermediate web stiffeners to plain CFS channel cross-sections provided minimum effect on the element flexural capacity. Most of previous studies on the cold-formed steel section members focused on the buckling of the members when they loaded by axial and bending loads. Lanc et al. (2015) have applied Bernoulli beam theory for bending, and Vlasov theory for beam torsion to illustrate the buckling behavior of thin-walled functionally graded sandwich box beam. A new analytical expression for computing web shear buckling of box sections was introduced by Bedair (2015), considering the flange restraints. Analytical formulas have developed to evaluate the global and local buckling strengths, to obtain solutions in a design constrained by geometric conditions. The results of their study indicated better flexural performance compared

* Corresponding author. Tel.: +2-013-322-8887; E-mail address: ahmed.mohamed@bhit.bu.edu.eg (A. Y. Kamal)

to the traditional lipped or plain channel sections. Ma et al. (2015), have optimized the CFS compression and bending members with respect to their capacity according to EC3 (2005).

Compared with traditional reinforced concrete structure, the encased beam has a higher bearing capacity and ductility. Besides, it is also an economic structure element and easily constructed compared to load capacity gained. Because of these characteristics, it is widely used in constructions such as high-rise buildings and bridges. The modern building has a higher demand for the construction height and span length. Encased beam, which takes the advantage of both concrete and cold-formed steel (CFS) members can raise the element load capacity and decrease the weight of the structure. Ammar et al. (2012), said that the high percentage of the steel area in encased beam improves the beam ductility. Based on the previous literature review the beneficial effect of using the CFS is obvious, in our paper, we aimed that encasing the cold-formed steel (CFS) members in concrete will restrict the local buckling of cold-formed steel section. In addition, providing multi-web section will decrease the web slenderness ratio, which has the direct effect to overcome the local buckling problem.

2. Material Properties

Eleven specimens were prepared and tested in Benha Concrete Laboratory, Benha Faculty of Engineering, Egypt. One of them was concrete beam reinforced by only upper and lower steel bars referred as reference beam. Ten specimens were enhanced by multi-web cold-formed section; with the same reference beam concrete dimensions.

All specimens were with full-scale beams loaded by mid-span concentrated load. All beam specimens had a square concrete cross-section with side length of 150 mm. The total concrete specimen length and the clear length are identical for all specimens, with 1500 mm and 1400 mm respectively, as shown in Fig. 1.

All specimens were reinforced by two bars with 12 mm diameter upper and lower (high tensile steel) as a tension and compression reinforcement, equivalent to reinforcement ratio of 0.02, with average yield strength of 37 kg/mm². The average elastic modulus for all reinforcements was 20900 kg/mm². For shear resistance, closed mild steel stirrups with 8 mm diameter were provided and equally distributed with space of 200 mm (center to center) along the specimen length; stirrups existence makes a good engagement to the longitudinal bars, and enhances the beam ductility, as shown in Fig. 2. The concrete cover was taken as 10 mm all over the beam section. The average laboratory concrete compressive strength was 3.1 kg/mm², with average concrete volume weight of 2.3 kg/cm³; as a result of laboratory tests.

Table 1 shows the details of the experimental program, to evaluate and monitoring the studied parameters effect on the structural behavior of the encased beams using multi-web cold-formed steel sections. Specimens were divided into three groups with three variables, first group with different numbers of webs, the second group with variable web normalized height (η) (which defined as the cold-formed steel members height divided by the concrete section height) and the third one with variable cold-formed steel sections normalized length (λ) (which defined as the cold-formed steel members length divided by the concrete section length).

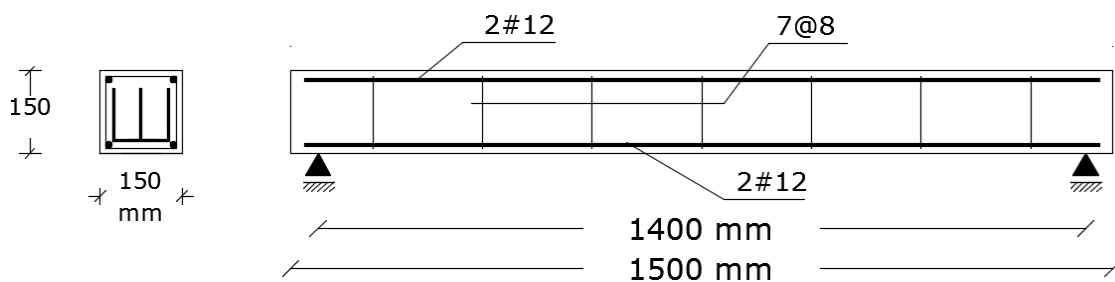


Fig. 1. Specimen dimensions.



Fig. 2. Upper and lower specimen reinforcement.

Table 1. Specimen details.

	Specimen Code*	Cold-formed steel section				Normalized height ($\eta = h_s/h$)	Normalized height ($\lambda = L_s/L$)
		h_s (mm)	b_s (mm)	L_s (mm)	Web Number		
Group A	MWS1-1	---	110	1450	---	0	1
	MWS1-2	95	110	1450	1	0.63	1
	MWS1-3	95	110	1450	2	0.63	1
	MWS1-4	95	110	1450	3	0.63	1
	MWS1-5	95	110	1450	4	0.63	1
	MWS1-6	95	110	1450	5	0.63	1
Group B	MWS2-1	---	110	1450	---	0	1
	MWS2-2	50	110	1450	3	0.33	1
	MWS2-3	70	110	1450	3	0.47	1
	MWS2-4	95	110	1450	3	0.63	1
Group C	MWS3-1	95	110	460	3	0.63	0.33
	MWS3-2	95	110	930	3	0.63	0.66
	MWS3-3	95	110	1450	3	0.63	1

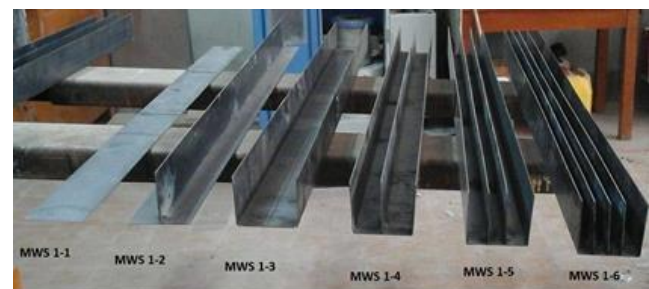
* MWSx-x: Multi-Web Section (Group number-Specimen number)

Ten specimens were divided to three groups, (MWS1, MWS2 and MWS3), with different number of web (0, 1, 2, 3, 4 and 5) equally spaced web, different web height of (0, 50, 70 and 95 mm), and different (CFS) length (460, 930, and 1450 mm), as shown in Figs. 3(a-c). All the cold-formed steel section (CFS) was with constant thickness of 2 mm, and average yield strength of 28 kg /mm². The centroids of both the cold-formed steel section and the concrete specimen cross section were vertically coincident.

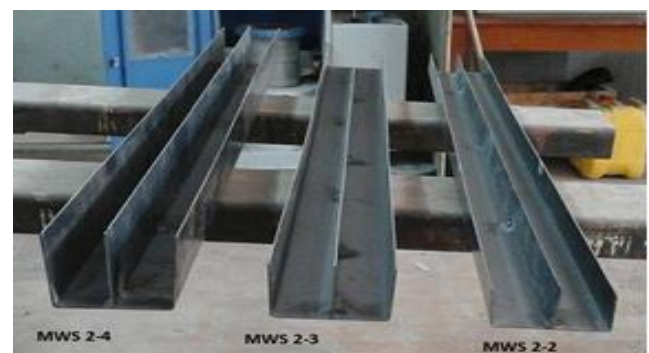
3. Test Setup

As shown in Fig. 4, specimens were simply supported by two concrete blocks on a loading frame. All specimens were loaded by mid-span vertical load, applied by a 100 t hydraulic jack capacity connected to digital recording apparatus. Vertical displacements were recorded by Linear Variable Differential Transformer (LVDT's) with magnetic base, distributed along the specimen length. The (LVDT's) were distributed as two in the right side of the specimen (LVDT 1, 2), one under the concentrated load (LVDT 3) and one at mid-span between the applied concentrated load and the left support (LVDT 4), as shown in Fig. 4.

To measure the longitudinal strain at the mid-span of the specimen, strain gauge with a length of 10 mm were pasted on the (CFS) mid-span, and covered by water-proof material, as shown in Fig. 5. All results (load, vertical deflections, and strain) were automatically recorded by a computer system and saved as Excel file format.



(a) Group A



(b) Group B



(c) Group C

Fig. 3. Groups details.

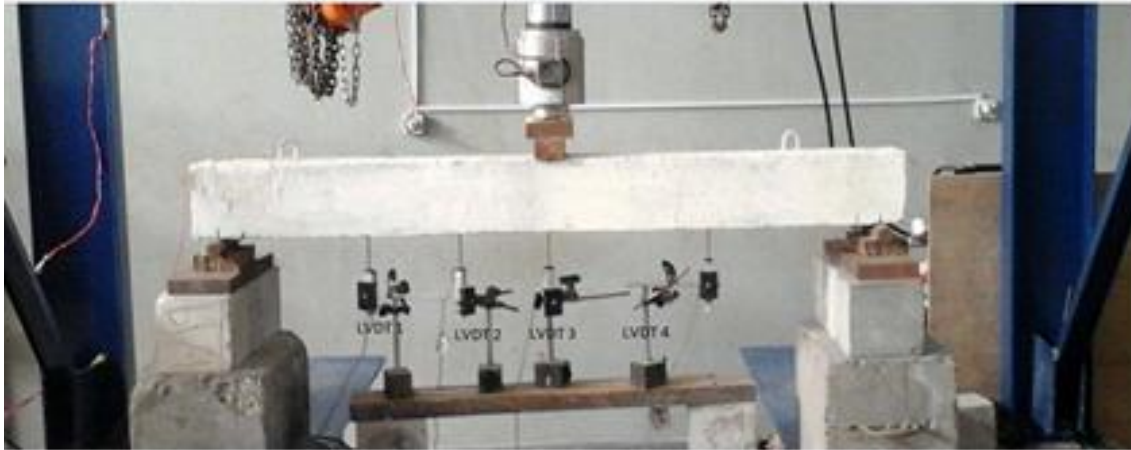


Fig. 4. The linear variable differential transformer distribution.



Fig. 5. Mid-span strain gauge.

4. Results and Discussion

4.1. Cracking and failure load

The reference beam specimen failed in ductile flexure mode, with a beam load capacity ($P_f=4100$ kg), and with cracking load ($P_{cr}=2700$ kg), Table 2. According to the observation for the reference beam, flexure concrete first

cracks initiated at 66% of the beam load capacity at the bottom zone and extended up to about 85% of the beam height, followed by the first diagonal crack at about 92% of the beam load capacity. All cracks grew in size and number toward the applied load until failure, as shown in Fig. 6.

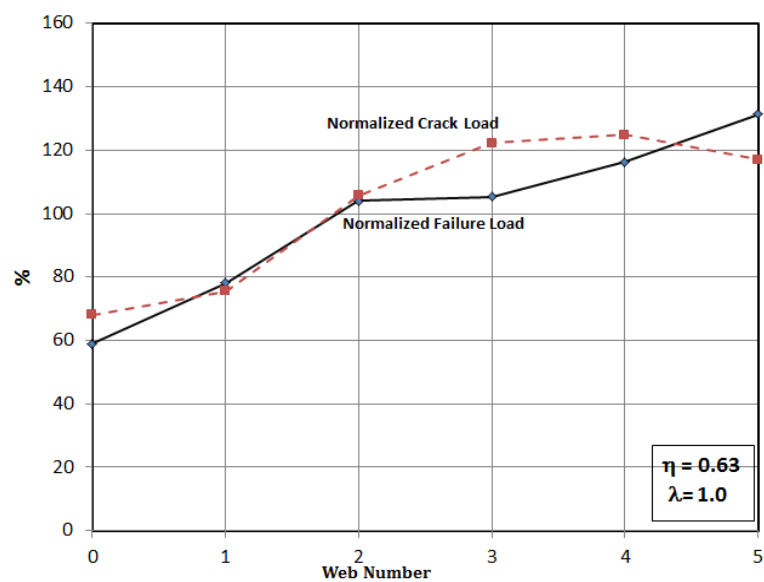
Fig. 7 represented the first cracking initiation load and the failure load as a percentage of that of reference beam (normalized load).

Table 2. Specimens' failure mode and ductility.

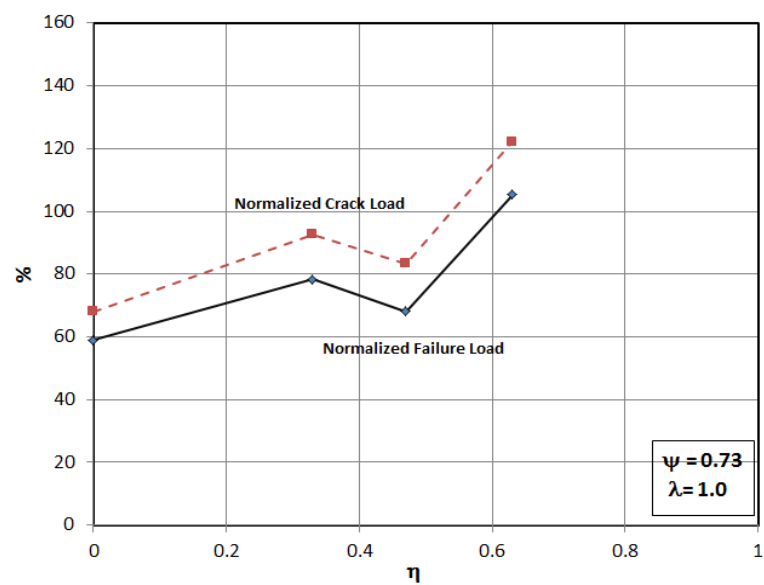
Specimen Code	Cracking load P_{cr} (kg)	Failure load P_f (kg)	Cracking factor ($F_{cr} = P_{cr}/P_f$) (%)	Mode of failure	Deflection at first crack Δ_{cr} (mm)	Deflection at failure Δ_f (mm)	Factor of ductility F_d
MWS1-1	1840	2425	76	Flexural / Splitting	2.10	42.19	15.2
MWS1-2	2040	3210	64	Flexural / Splitting	3.17	43.73	13.8
MWS1-3	2855	4275	67	Local buckling	2.7	33.03	9.7
MWS1-4	3300	4330	76	Flexural / Local buckling	4.07	19.24	4.72
MWS1-5	3370	4780	70	Flexural / Local buckling	4.66	20.56	4.41
MWS1-6	3160	5400	59	Support bearing failure	4.32	11.95	2.77
MWS2-1	1840	2425	76	Flexural / Splitting	2.10	42.19	15.2
MWS2-2	2500	3220	78	Flexural / Local buckling	4.07	32.76	8.05
MWS2-3	2250	2800	80	Local buckling	3.45	34.2	9.91
MWS2-4	3300	4330	76	Flexural / Local buckling	4.07	19.24	4.72
MWS3-1	2960	4800	62	Flexural / Shear	5.02	23.14	4.61
MWS3-2	3160	4800	66	Flexural / Shear	4.15	15.42	3.72
MWS3-3	3300	4330	76	Flexural / Local buckling	4.07	19.24	4.72
Reference beam	2700	4110	66	Flexural	4.8	31.2	6.5



Fig. 6. Reference beam crack pattern.



(a) Group A



(b) Group B

Fig. 7. (continued)

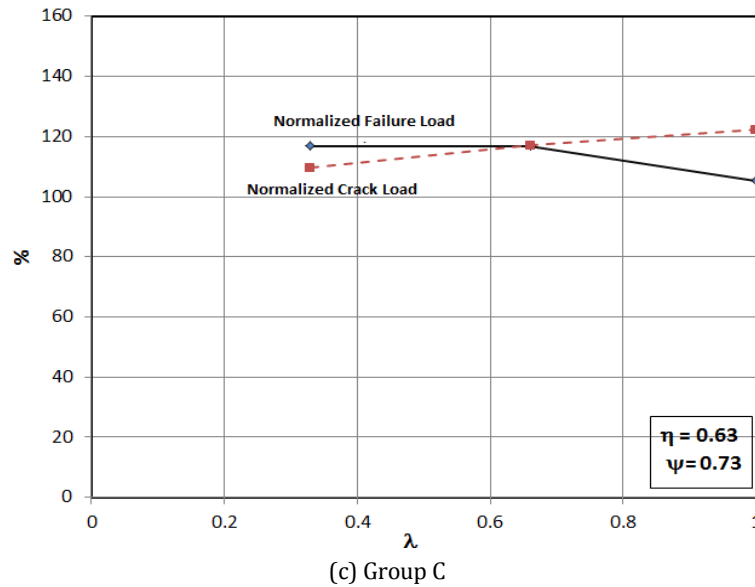


Fig. 7. Normalized crack and failure loads.

Providing the multi-web sections (MWS) with ($\psi=0.73$, $\eta=0.63$, $\lambda=1.0$), (ψ defined as the cold-formed steel members width divided by the concrete section width) and with different number of web (MWS1-3, MWS1-4 and MWS1-5), increase the beam load capacity by (4, 5, and 16% respectively) compared with the reference beam. Those models shared in similar failure mode, initiation of bottom flexure concrete cracks followed by concrete side crushing due to local buckling occurred in the (CFS) web; as a result of relatively small concrete cover resist the (CFS) web local buckling, as shown in Figs. 8(c-e). While shear splitting failure led the models with no web and one centered web (MWS1-1, MWS1-2) to fail with a load capacity less than the reference beam by (41, 22% respectively), as shown in Figs. 8(a-b). Sudden failure (without noticeable concrete flexure cracks

observation), due to support bearing failure was observed for model (MWS1-6), with noticeable increase of 31% in the beam load capacity compared with the reference beam, as shown in Fig. 8(f). Multi-web sections in models (MWS1-3, MWS1-4, MWS1-5, & MWS1-6) delayed the initiation of concrete cracks by (6, 22, 25, and 17%) respectively, with respect to that of reference beam, while for models (MWS1-1, MWS1-2) the concrete cracks initiated early by (32, 24%) respectively, than of that in reference beam, as shown in Fig. 7(a).

Average decreasing by (25, 35% in average) in the mid-span strain was recorded for models (MWS1-5 and MWS1-6) compared with model with one centered web. Beam with no web and one centered web cold-formed steel section fail before the cold-formed section reach yield, as shown in Fig. 9.



(a) MWS1-1



(b) MWS1-2

Fig. 8. (continued)



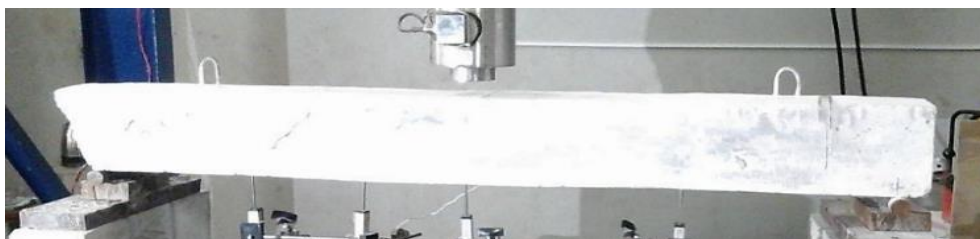
(c) MWS1-3



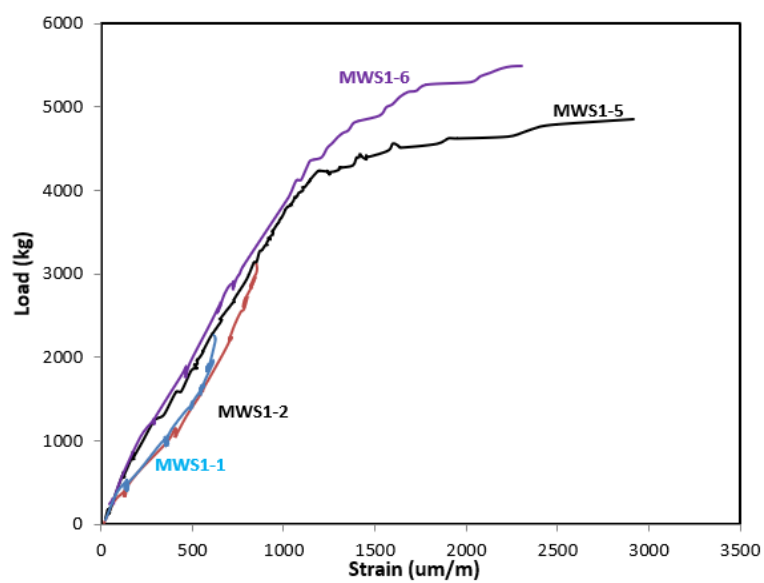
(d) MWS1-4



(e) MWS1-5

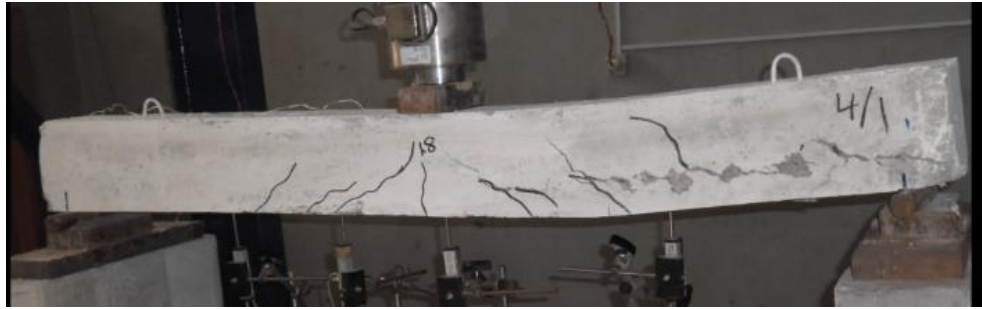


(f) MWS1-6

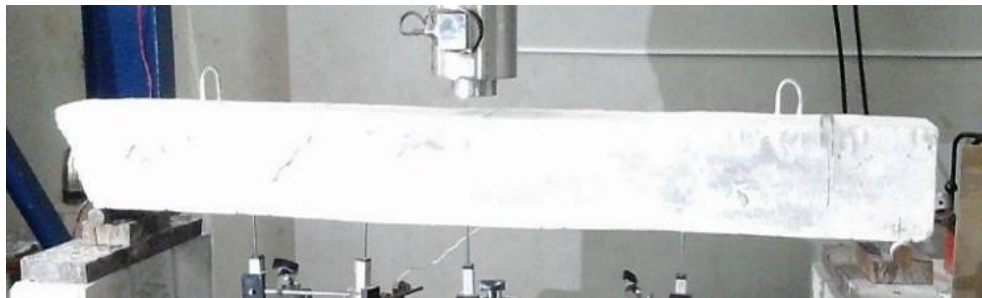
Fig. 8. Failure mode for models (group A).**Fig. 9.** Mid-span strain (Group A).

Web local buckling of models with three-web section, constant normalized width and length ($\psi=0.73$, $\lambda=1.0$), and with variable normalized height (η), led the models (MWS2-2, MWS2-3) to fail early, with decreasing in the load capacity by (22, 32% respectively), compared with the reference beam, as shown in Figs. 10(b-c). While shear-splitting failure led the model (MWS2-1) to fail with a decreasing percentage of 41%, in beam load capacity with respect to the reference beam, as shown in Fig. 10(a). Model (MWS2-4) with three-web section

($\eta=0.63$, $\psi=0.73$, $\lambda=1.0$) recorded a little increase by 5% in the load capacity compared with the reference beam with local buckling failure, as shown in Fig. 10(d). As Models (MWS2-1, MWS2-2 and MWS2-3) reached failure load early than reference beam, the concrete cracks initiation for those models were initiated early by (22, 8 and 17%) respectively, compared with the reference beam. While the concrete cracks initiation for model (MWS2-4) delayed by 22% than that of reference beam, as shown in Fig. 7(b).



(a) MWS2-1



(b) MWS2-2



(c) MWS2-3



(d) MWS2-4

Fig. 10. Failure mode for models (group B).

Providing the three-web cold-formed steel section ($\eta=0.63$, $\psi=0.73$), with different values of normalized length (MWS3-1, MWS3-2 and MWS3-3) increase the beam load capacity by (17, 17, and 5%, respectively), compared with the reference beam. Decreasing the three-web cold-formed steel section length for specimens (MWS3-1 and MWS3-2), force the model to fail

with initiation of flexure cracks, ended with brittle shear failure, as shown in Figs. 11(a-b). While specimen (MWS3-3) with three-web cold-formed steel section and full length, failed due to web local buckling. The concrete cracks initiation delayed by (22, 17, and 10%) for models (MWS3-1, MWS3-2 and MWS3-3), respectively.



(a) MWS3-1



(b) MWS3-2



(c) MWS3-3

Fig. 11. Failure mode for models (group C).

Specimens (MWS3-1 and MWS3-2) fail before the cold-formed section reach yield, due to the model brittle shear failure. Increasing by (80 and 35%) (In average) in the mid-span strain for a specimen (MWS3-3, MWS3-2 respectively), with respect to specimen (MWS3-1) was observed, Fig. 12.

In aim of declare the relationship between the failure load and cracking load, cracking factor (F_{cr}), was introduced as the percentage of the load at which first concrete crack initiated to the failure load. The cracking factor for the reference beam was 66%.

For the first group this factor was approximately the same as the reference beam for models (MWS1-2, MWS1-3), and was reduced to (59%) for model (MWS1-6) which provided good announcing before failure, while this factor increased to (76, 76 and 71%) for models (MWS1-1, MWS1-4 and MWS1-5) respectively as shown in Fig. 13(a). The cracking factor increased for the second group to 78% in average for models (MWS2-1, MWS2-2, MWS2-3 and MWS2-4) respectively, as shown in Fig. 13(b). The cracking factor for the third group was approximately the same as the reference beam for models (MWS3-1, MWS3-2), increased to 76% for model MWS3-3, Fig. 13(c).

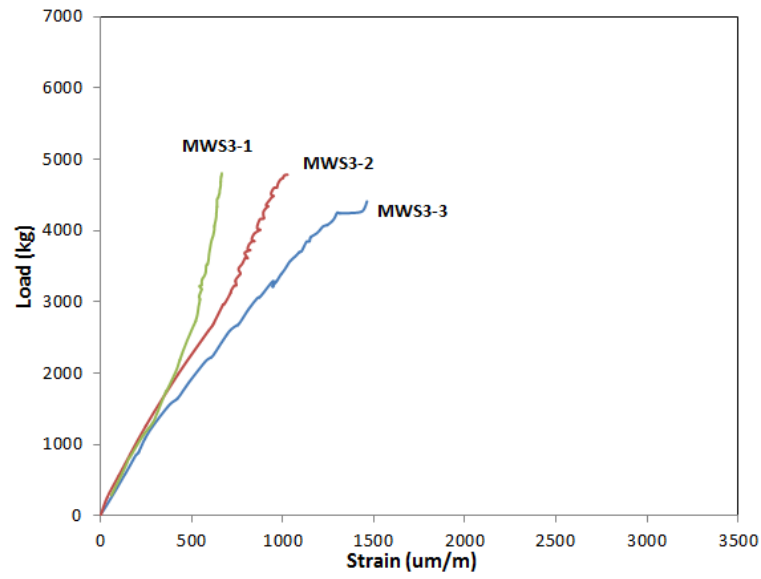
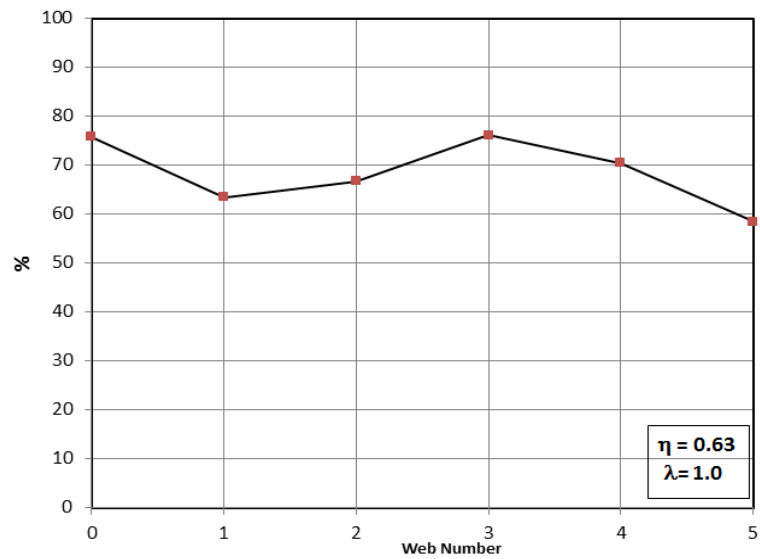
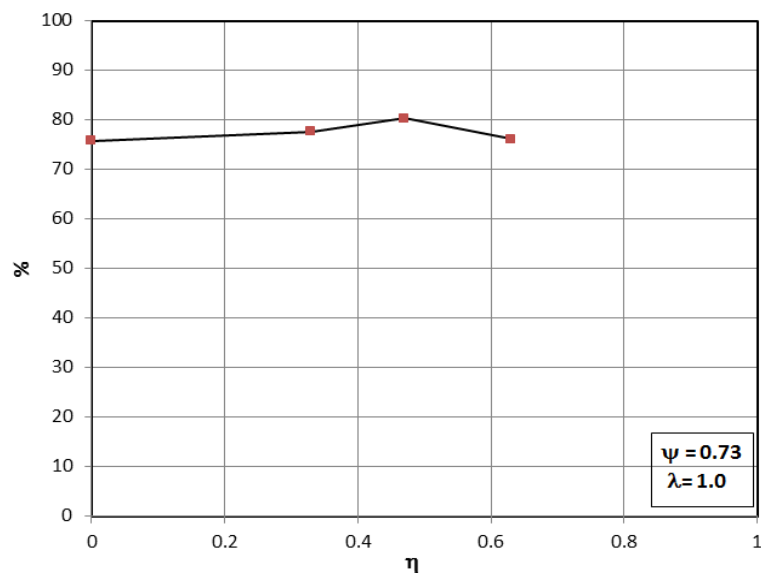


Fig. 12. Mid-span strain (Group C).



(a) Group A



(b) Group B

Fig. 13. (continued)

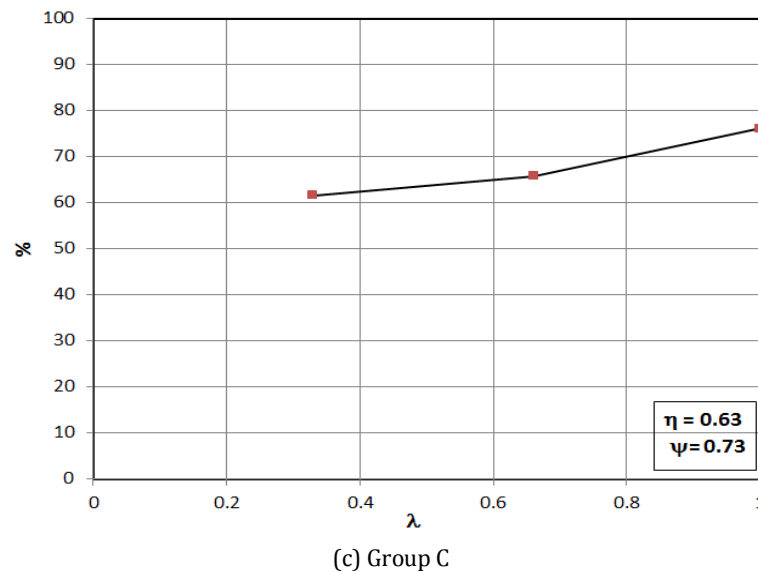


Fig. 13. Cracking factor.

4.2. Deflections

The deflection-load curves for models with one-center web (MWS1-2) and that with five webs (MWS1-6) at the beam mid-span (dial 3), were plotted, and compared with that of the reference beam. The curves illustrate the ductile (flexure) failure for both reference beam and model with one-center web, while increasing the number of webs to five changes the mode of failure to brittle failure. The curves also indicate that increasing the number of webs to five decreases the deflection by about 35% (in average) with respect to reference beam, as shown in Fig. 14(a). Fig. 14(b) represents the deflection-load curves for group A, the figure indicates decrease in deflection by 33% in average for models with 3, 4 and 5 webs with respect to reference beam.

Fig. 14(c) represents the deflection-load curves for group B, the figure indicates decrease in deflection by 40% in average for model (MWS2-4), with no noticeable change for other models.

Using of the three-web cold-formed section with total length, two-third, and one-third the concrete beam length

decreases the deflections by average values of 33, 30, 5% respectively with respect to reference beam, Fig. 14(d).

In addition, the deflected shapes for specimens (MWS1-2, MWS1-6), along the beam length were plotted at a certain load level (linear stage), and was compared with the deflected reference beam, as shown in Fig. 15(a). The figure shows that there was a decrease of (7, 23% in average), in the beam deflection for specimens (MWS1-2, MWS1-6) respectively, with respect to that of reference beam. From that, the Multi-web sections shared in decreasing the deflections more than that of reference beam.

The deflected shapes for specimens (MWS3-1, MWS3-3) were plotted along the beam length at the same load level (linear stage), and was compared with that of reference beam, as shown in Fig. 15(b). The figure shows that there was a decrease of (8, 38% in average), in the beam deflections for specimens (MWS3-1, MWS3-3) respectively, with respect to that of reference beam. From that, the full-length cold-formed steel section shared in decreasing the deflections more than that with less length.

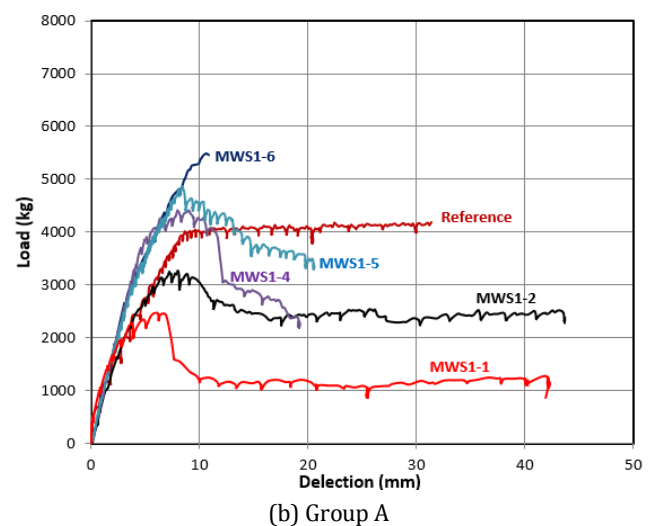
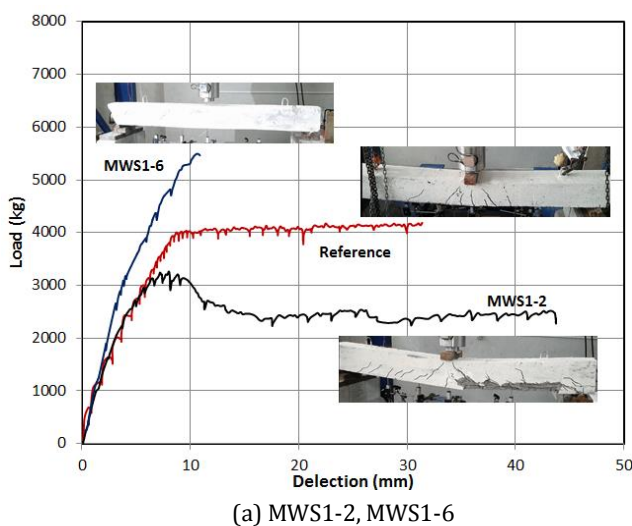


Fig. 14. (continued)

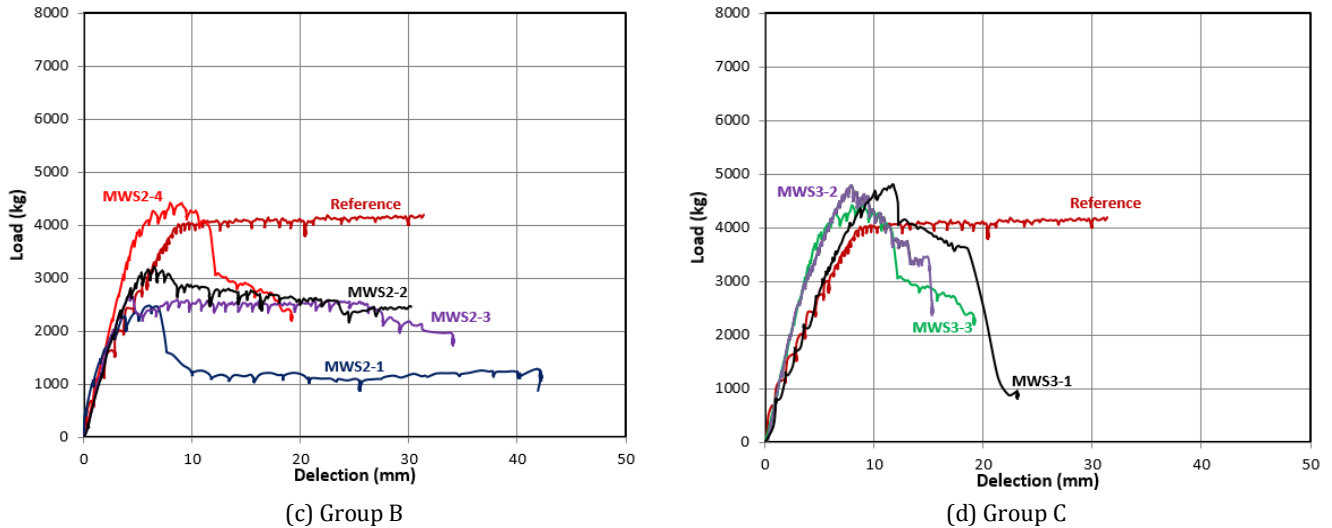


Fig. 14. Deflection-load curves.

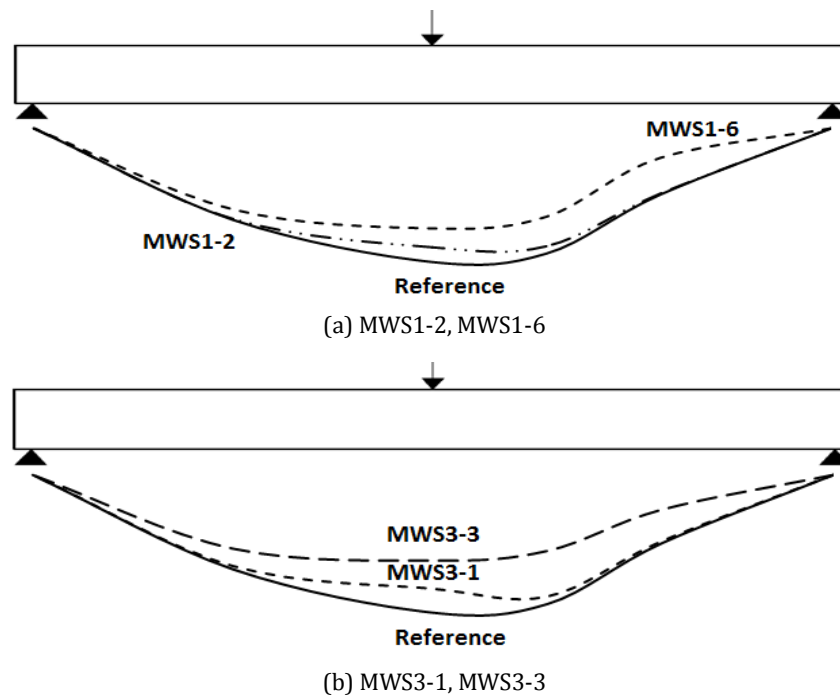


Fig. 15. Deflected shapes.

4.3. Factor of ductility

By applying the fracture mechanics concepts, there could be a safety margin against failure with reasonable reliability, also a safety margin for prediction the beam failure. Factor of Ductility (F_d) is defined as the ratio of mid-span deflection at beam failure to that at the first concrete crack, the reference beam factor of ductility was 6.5, as shown in Table 2.

Figs. 16(a-c) shows (F_d) variation with the web (number, height, and length) respectively. It declared that the ductility factor decreased as the web number and normalized height increased, while variation of the normalized length had no noticeable effect on the factor of ductility (all were less than that of reference beam). The ductility factor was observed to be the highest for models (MWS1-1 and MWS1-1), then the reference beam.

5. Conclusions

Through the experimental research on the multi-web cold-formed steel section structural behavior, the following conclusions were obtained:

- Providing a multi-web cold-formed steel section increase the beam load capacity with a significant value and make good benefits of using cold-formed steel section.
- Providing a multi-web cold-formed steel section decrease the beam deflection with a significant value.
- Increasing the number of webs for the cold-formed steel section has a significant effect in decreasing the stress on the cold-formed steel section.
- Shear splitting failure can be avoided by using end web sections.
- Local buckling in the cold-formed steel governs the structural element failure.

- Reducing the multi-web cold-formed steel section length (less than two-thirds of beam length), increase the beam load capacity with a significant value, than using full length, but led to brittle shear failure.
- Reducing the multi-web cold-formed steel section length (two-thirds of beam length), decrease the beam deflections approximate the same of that with full-length with a significant value.

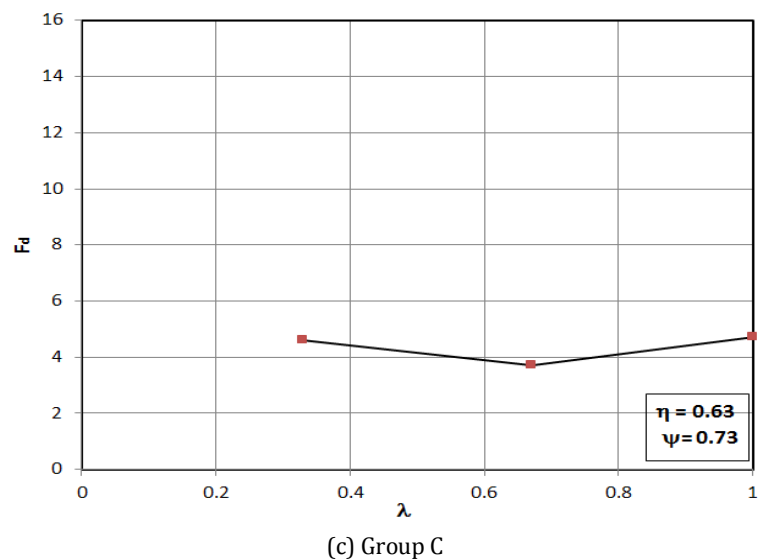
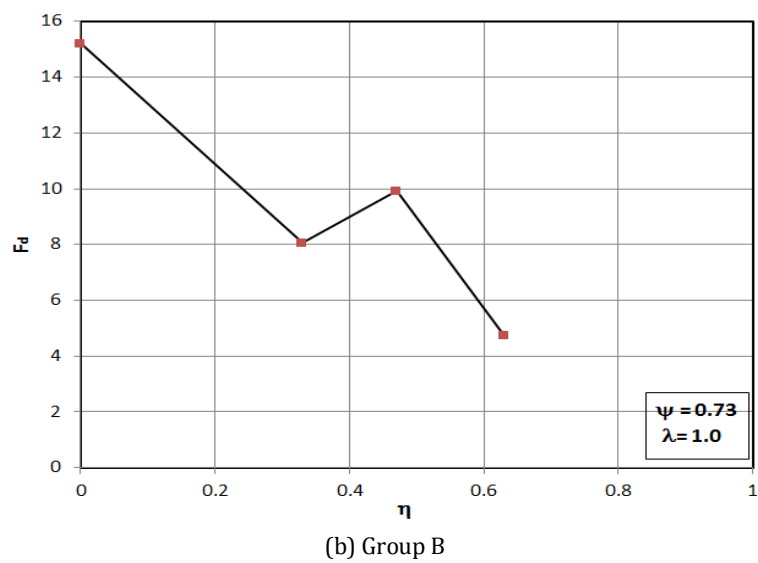
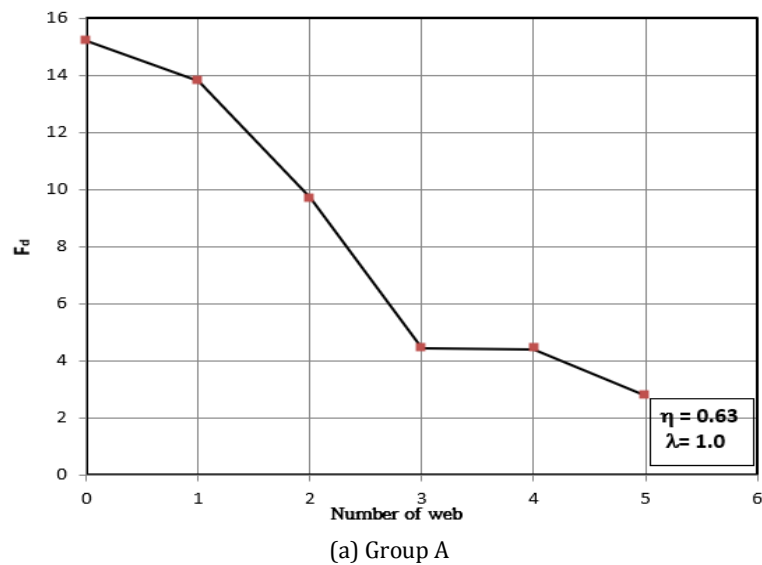


Fig. 16. Factor of ductility.


REFERENCES

- Ammar A, Saad N, Wael S (2012). Strength and ductility of concrete encased composite beams. *Engineering and Technology Journal*, 30, 2701-2714.
- Bedair O (2015). Design expression for web shear buckling of box sections by accounting for flange restraints. *Journal of Constructional Steel Research*, 110, 163–169.
- CEN, Eurocode 3 (2005). Design of Steel Structures, Part1-3: General Rules — Supplementary Rules for Cold-formed Steel Members and Sheeting. European Committee for Standardization, Brussels.
- Gilbert BP, Savoyat TJM, Teh LH (2012b). Self-shape optimisation application: optimisation of cold-formed steel columns. *Thin-Walled Structures*, 60, 173–184.
- Gilbert BP, Teh LH, Guan H (2012a). Self-shape optimization principles: optimization of section capacity for thin-walled profiles. *Thin-Walled Structures*, 60, 194–204.
- Hancock GJ (2007). Design of Cold-formed Steel Structures, 4th Edition. Australian Steel Institute, North Sydney, Australia.
- Lanc D, Vo TP, Turkalj G, Lee J (2015). Buckling analysis of thin-walled functionally graded sandwich box beams. *Thin-Walled Structures*, 86, 148-156.
- Leng J, Guest JK, Schafer BW (2011). Shape optimization of cold-formed steel columns. *Thin-Walled Structures*, 49, 1492–1503.
- Liu H, Igusa T, Schafer B (2004). Knowledge-based global optimisation of cold-formed steel columns. *Thin-Walled Structures*, 42, 785–801.
- Ma W, Becque J, Hajirasouliha I, Ye J (2015). Cross-sectional optimization of cold-formed steel channels to Eurocode 3. *Engineering Structures*, 101, 641 - 651. ISSN 0141-0296
- Madeira JFA, Dias J, Silvestre N (2015). Multi-objective optimisation of cold-formed steel columns. *Thin-Walled Structures*, 96, 29–38.
- Moharrami M, Louhghalam A, Tootkaboni M (2014). Optimal folding of cold-formed steel cross sections under compression. *Thin-Walled Structures*, 76, 145–156.
- Pham SH, Pham CH, Hancock GJ (2014). Direct strength method of design for shear including sections with longitudinal web stiffeners. *Thin-Walled Structures*, 81, 19-28.
- SFIA (2012). Technical Guide for Cold-Formed Steel Framing Products. Steel Framing Industry Association, United States of America.
- Wang B, Bosco GL, Gilbert BP, Guan H, Teh LH (2016). Unconstrained shape optimisation of singly-symmetric and open cold-formed steel beams and beam columns. *Thin-Walled Structures*, 104 54–61.
- Ye J, Hajirasouliha I, Becque J, Pilakoutas K, (2016). Development of more efficient cold-formed steel channel sections in bending. *Thin-Walled Structures*, 101, 1-13.
- Yu WW (2010). Cold-Formed Steel Design, 4th Edition. Wiley, Hoboken, United States of America, NJ.



Research Article

Properties of self-compacting concrete containing granite dust particles

Joseph Abah Apeh * 

Department of Building, School of Environmental Technology, Federal University of Technology, Minna, Nigeria

ABSTRACT

In the course of production in the Granite Industry, a lot of quarry dust wastes is generated which is either heaped at sites causing environmental and health hazards or dumped in landfills causing ecological problems. It is imperative to evolve a viable option for disposal so to rid the environment of this menace. This study investigated the use of quarry dust particles (QDP) generated from the granite industry as a cement replacement in self-compacting concrete (SCC). The experimental program was carried out in two phases: the first phase optimized the amount of QDP as replacement of Portland cement (PC) with acceptable flow-ability. The second phase evaluated the fresh and hardened properties of SCC which include tests on slump flow, J-ring and L-box to determine filling, passing abilities of SCC while compression and splitting tensile tests were conducted to determine the compressive and splitting tensile strengths, respectively. Test results show that at 20% replacement of cement with QDP, the SCC-QDP mixes has a slump ranged from 642 to 730 mm compared with 578 mm for SCC mix, a compressive strength of 37 N/mm² compared with 30 N/mm² for SCC. This was enhanced by QDP which filled the voids between the coarse grains of cement and water molecules which facilitated the flow ability of the mixes and then at later ages reacted with liberated calcium hydroxide from cement hydration to enhance the strength of the mixes. The results then indicated that QDP can be used to replace PC up to 20% by mass of PC in the production of SCC without adverse effect on both fresh and hardened properties. This results also show that QDP, a suitable material for partial replacement of PC in SCC production, can be used to reduce demand for cement thus reducing carbon dioxide emission and also solve other environmental problems.

ARTICLE INFO

Article history:

Received 30 January 2019

Revised 30 April 2019

Accepted 22 June 2019

Keywords:

Self-compacting concrete

Quarry dust fine powder

Fresh and mechanical properties

Pozzolanic reaction

Compressive strength

1. Introduction

Among the most widely manufactured and used materials, concrete is second to none. Because of this fact, it has to fulfill a wide range of requirements in both fresh and hardened state. Since in most cases, the fresh properties affect the quality of the hardened state and by extension the durability, it is imperative to attain a correct mix proportion so as to remain homogeneous during placing and after compaction in order to avoid bleeding and segregation. Self-compacting concrete (SCC) is concrete cast and compacted without any vibrational means which flows

under its own weight. SCC mixes increase productivity, reduce noise pollution and improve construction quality. Furthermore, it has both filling, passing ability and high resistance to segregation during transportation and placing. To achieve this the concrete requires high slump with the aid of super-plasticizer (SP) added to the concrete mixture and its mix proportioning. The use of SP is imperative for the production of a high fluid concrete mix with high powdery content materials (viscosity modifying agents) is required to enhance sufficient stability/cohesion of the mixture hence reducing bleeding and segregation and settlement (Wenzhong and Gibbs, 2005).

* Corresponding author. Tel.: +234-805-125-4651 ; E-mail address: apehjoe@futminna.edu.ng (J. A. Apeh)

ISSN: 2548-0928 / DOI: <https://doi.org/10.20528/cjcr.2019.02.002>

The work of Ouchi et al. (2003) has shown that it is beneficial to use SCC because of its improvement in homogeneity of concrete production and its excellent surface quality without honey combs. The mix proportioning is achieved by a suitable selection and proportioning of raw materials, reduction of water/powder ratio, increasing paste volume, controlling the total volume of coarse aggregates and its maximum particle size (EF-NARC, 2005) and other constituents to achieve the required level of material performance both in the fresh and hardened state. Consequently, the powdery materials content is high, resulting in high volume content of cement which in turn leads to a higher temperature rise, increase in heat of hydration, creep, shrinkage and increase in cost which can be off-set with the use of mineral admixtures. Industrial by products such as ground granulated blast furnace slag, Limestone powder and fly ash are commonly used mineral admixtures (Poon and Ho, 2004), similarly, other industrial by product such as granite dust particles, if its use in SCC is proven to be appropriate can serve as a solution to its disposal problem confronting the granite industry.

Granite dust particles is obtained when rocks of granite origin are crushed to produce aggregates on quarry sites. Granite particles is fine aggregates less than 4.75 mm in diameter. It is also obtained from granite cutting and polishing industry which yields fine granite particles which is disposed in nearby areas without any treatment. Granite dust particles as an admixture when used in SCC can sufficiently improve workability of SCC (Sahmarain et al., 2006; Uysal et al., 2011) and also reduce the amount of SP necessary to achieve a given property as obtained by Sonebi et al., (2000). Hafez et al. (2014) has pointed out in their study that the effect of mineral admixture on admixture requirements is significantly dependent on their particle size distribution, shape and surface characteristics. This shows that a cost effective SCC design is obtained upon the incorporation of reasonable amounts of mineral admixtures such as limestone powders (LP), Ballast powder, (BP) and marble powder (MP) as indicated by the work of Uysal et al. (2011). Hafez et al. (2014) further established that the addition of MP is the best among the aforementioned mineral admixtures which improved SCC fresh properties such as slump-flow, T_{50} time, L-box ratio and J-ring.

Results of studies conducted on the effects of mineral admixtures as filler materials on the properties of SCC improved the workability with reduced cement content, which in turn led to the reduction of hydration, thermal and shrinkage cracking as seen in the works of Ye et al., 2007; and Poppe and Schutter (2005). The work of Belaidi et al. (2012) shows that at a constant water / binder ratio and SP content, cement substitution by the use of natural pozzolan and MP has no negative effects on workability of SCC. Stone dust and other industrial by-products have been used as filler materials in SCC (Sahmarain et al., 2006). The incorporation of quarry dust (QD) in SCC improves its workability, increase in strength and durability against chemical attack (Manjul and Premalatha, 2006). Manju et al. (2014) studied the effect of partially reducing quantities of cementitious materials with MP on the compressive, tensile as well as

flexural strength of mortar and concrete. The compressive strength of sample cubes increased with increase in waste content of MP up to 12.5% and then decreased with further increase in MP. This confirms the earlier work of Baboo et al. (2011) on the influence of MP in concrete.

The work of Vijayalakshimi et al. (2013) on durability properties of concrete shows that QD can replace sand up to 15% without any adverse effect on the durability properties of concrete. The work of Suma (2016) also show that QD as a filler is a suitable material for the production of SCC. Gowda et al (2000)'s work also show that fresh and hardened properties of SCC improved when QD was used to replace sand at varying proportions. For normal concrete, Allam et al. (2016) studied the effect of partial replacement of cement with granite waste on the mechanical properties of concrete. Test results showed that with 5% granite replacement of cement, splitting tensile strength was 20% higher, flexural strength was 19% lower with bond strength also slightly lower by 1% when compared with control values. Working along the same line of thought, Kumar et al. (2013) increased QD replacement of cement proportions of 10, 20, 25, 30, 35 and 40% respectively. From experimental results, they reported that 25% partial replacement of cement with QD showed improved hardened properties of normal concrete. It is worthy to note that granite waste particles used in these studies were sieved through sieve size 300 μm and through sieve size 4.75 mm and the concrete is normal concrete.

When granite fines as supplied is compared with Limestone powder, the work of Ho et al. (2002) on both paste and concrete confirmed that granite fines incorporated in SCC required a higher dosage of SP for similar yield stresses and other rheological properties. But one must take cognizance of the fact that granite fines being a waste material, its properties will vary over time and also dependent on parent rock and mode of generation such as crushing, cutting or sawing. Dehwah (2012) has also reported that the mechanical properties of SCC incorporated with QDP is better than those of SCC with silica fume (SF) with QDP or only Fly ash (FA). He further pointed out that it is more economical to use QD alone especially in regions where SF and FA are not readily available locally and has to be imported.

From the works of researchers reviewed so far, it shows that the flow properties of SCC depend on powder particle size, shape, surface morphology and internal porosity in addition to other factors such as mixing regimes, sequence of admixtures addition, and water / SP content (Rizwan and Bier, 2013). It is also clear that the focus of most studies was on the utilization of marble and granite powder as fillers in concrete and also as a sand replacement material. However, this study will focus on the application of QDP as a replacement of cement in the production of SCC. This is because mixes containing MP and QD required the use of SP otherwise more quantity of water will be required for similar workability, which consequently reduces strength. On the other hand, the high fines of QD may be beneficial for providing good cohesion to SCC, if it is used as mineral additive (Uysal and Sumer, 2011). However, more studies are required to evaluate the behavior of SCC containing QDP of high fineness. It is hypothesized that the finer particle

sizes of QDP would further increased the pozzolanic reactivity between cement and the former during secondary hydration process. Therefore, this paper evaluated the effect of partial replacement of cement with QDP on the fresh and mechanical properties of SCC. The fresh and hardened properties of SCC was investigated and compared with those of control mix produced with plain Portland cement.

2. Materials and Method

2.1. Materials

Concrete mixes were prepared with Portland cement CEM 1 42.5 N conforming to BS EN 196-6 (1997). Fine aggregates used was natural siliceous sand with a fineness modulus of 3.0 and specific gravity of 2.39. Blended crushed granite aggregates of 19 mm and 10 mm nominal sizes with specific gravities of 2.69 and 2.60 were used. QDP was used as a partial replacement of cement. It was obtained from a local quarry site in Minna, Niger state Nigeria. The sieve analysis test for the sample (as supplied) is shown in Table 2. The sample used for the study was sieved and the particle size distribution (PSD) is shown in Fig. 4. Portland cement classified as CEM 1 42.5 N was used for the study. The physical and chemical composition of the materials are shown in Tables 1 and 4.

2.2. Mix proportion

A fixed water/binder ratio of 0.40 was used while the dosage of the SP was slightly altered to obtain the desired slump-flow for the SCC; maintaining consistency with QDP replacement of cement. By reducing contents of the blended coarse aggregates (19 mm and 10 mm based on packing density approach) with corresponding fine aggregates and conducting trial tests on fresh properties of SCC, a constant coarse / fine aggregate ratio of 0.87 was used for all the mixtures for the study (Table 3). An SP (Master Glenium ACE 456), a

Table 1. Properties of cement and quarry dust particles (QDP).

Property	Cement	QDP
Colour	Gray	Off-white
Specific gravity	3.15	2.19
Specific surface area (cm ² /g)	3000	4580
Soundness (mm)	4.8	
Setting time (mins)		
Initial	161	170
Final	202	261

Table 2. Sieve analysis test result on QDP.

Sieve Size	% Passing
4.75 mm	100
2.36 mm	97.65
1.18 mm	81.15
600 µm	64.15
300 µm	46.75
150 µm	29.75
75 µm	69.68
Pan	5.72

high range water reducing admixture based on a newly developed poly carboxylate ether polymer was used for the study so as to enhance flow ability of SCC. It is a whitish to light brownish liquid with a specific gravity of 1.06, PH value of 4–7 at 23°C with a chloride content of less than 0.01%; and alkali content (Na₂O equivalent %) less than 3%. It conforms to EN 934–2 and ASTM C494, Type A, E, and F. A cement content of 400 kg/m³ was used for the study and percentage replacement of cement with QDP material was 0, 10, 20, 30 and 40% respectively. In all five concrete mixes were cast as shown in Table 3.

Table 3. Mix proportion of SCC (kg/m³).

Mix ID	Cement (kg/m ³)	QDP (kg/m ³)	Fine Agg. (kg/m ³)	Coarse Agg. (kg/m ³)	Water (kg/m ³)	SP (kg/m ³)	W/B lt/100kg
SCC	400	-	848	741	160	2.00	0.40
SCC-QD ₁₀	360	40	848	741	160	2.00	0.40
SCC-QD ₂₀	320	80	848	741	160	2.00	0.40
SCC-QD ₃₀	280	120	848	741	160	2.00	0.40
SCC-QD ₄₀	240	160	848	741	160	2.00	0.40

Table 4. Chemical composition of PC and QDP.

Material	Chemical Composition										
	SiO ₂	Al ₂ O ₃	Fe ₂ O ₃	MgO	CaO	Na ₂ O	K ₂ O	P ₂ O ₅	MnO	SO ₂	LOI
PC	19.92	4.72	3.58	1.84	65.72	0.93	0.52	0.054	0.46	8.97	1.86
QDP	72.7	13.28	2.19	0.78	1.44	2.45	5.70	0.12	0.17	0.13	2.07

2.3. Method

The study was conducted in two phases. Phase one was the optimization of the amount of QDP as a replacement to cement content at which the optimum paste content was attained with acceptable flow ability of SCC, J-ring and L-box test values which measured the passing abilities of the SCC. The second phase was the evaluation of the hardened properties of SCC in terms of compressive and splitting tensile strength tests. These tests were conducted in accordance with EFNARC (2005), BS EN 12350-8 (2010), ASTM C642 (2013) and BS 1881: Part 3, respectively.

The slump flow test measures the filling ability of the fresh SCC. It is used to assess the horizontal free flow of SCC in the absence of obstructions, its ability to fill Formworks of structural elements with ease. The required SCC constituents (Table 3) was dry-mixed, then 70% of required water was gradually added and mixed thoroughly for 3 minutes and finally, remaining 30% of water was mixed with the required SP content, added to the concrete and mixed again for 2 minutes. The mix was then scooped into the inverted slump cone without any compaction or vibration and flushed with a straight edge. The cone was vertically lifted and SCC flows horizontally on the mixing pad until it stops flowing. The average diameter of the concrete circle was used as a measure of the filling ability (Fig. 1). The test was also used to measure the resistance to segregation in the SCC mixes tested, which can be detected by virtual inspection of periphery of the mix after it stopped flowing. Segregation is indicated by the occurrence of a 'halo' of paste or uneven distribution of aggregates in the mix which was absent in any of the mix.



Fig. 1. Slump flow test measurement.

The passing ability of SCC was determined using the J-ring and L-box tests. Either of the tests measured the ability of the SCC mixes to flow through obstructions like reinforcement bars in form work of structural elements. The J-ring was placed on the mixing pad and the inverted slump cone was placed inside the cone and slump cone test carried out as aforementioned (Fig. 2a). The slump was measured after the concrete stopped flowing

through the ring which indicated the passing ability of the mix. Similarly, for the L-box test, the vertical section was filled with 12 Litres of fresh concrete for each SCC mix, allowed to stand for 30 seconds and the gate lifted for the concrete to flow into the horizontal section of the L-box. The height of the concrete at the end of the horizontal section is expressed as a ratio to that remaining at the vertical section (H_2/H_1) after the concrete stopped flowing. This indicated the passing ability for each of the SCC mix cast and tested (Fig. 2b).



(a) J-ring flow test



(b) L-box flow test

Fig. 2. Flow test measurement of passing ability.

The J-ring test also measures the passing ability of SCC cast through reinforcement bars spaced evenly. The slump flow cone placed in the J-ring was filled with SCC cast and lifted vertically above mixing pad to allow concrete flow horizontally through the J-ring. The diameter of the concrete circle which flowed through the ring was measured which indicated the passing ability of the mix tested. The J-ring flow spread and the unrestricted slump flow were compared for each mix. The difference between spread diameters, ($D_{\text{flow}} - D_{\text{ring}}$) were measured for the SCC mixes. On completion of fresh property tests, the SCC specimens were cast in steel moulds (100 mm x 100 mm x 100 mm) cubes and of cylindrical diameter

150 mm x 150 mm in height without compaction, covered with plastic sheets and kept in laboratory conditions for 24 hrs. The specimens were de-moulded and cured in a water tank for varying curing ages. The cube specimens were then tested for compressive strength with a compression testing machine with a capacity of 2000 kN taking into account that each reading is the average of three specimens. Splitting tensile strength was determined in accordance with the provisions in ASTM C496/C496M (2004).

3. Test Results and Discussions

The constituent properties of the SCC, its fresh properties in terms of filling and passing abilities, and the hardened properties in terms of compressive and splitting tensile strengths and that due to replacement of PC with QDP in the concrete is discussed as follows:

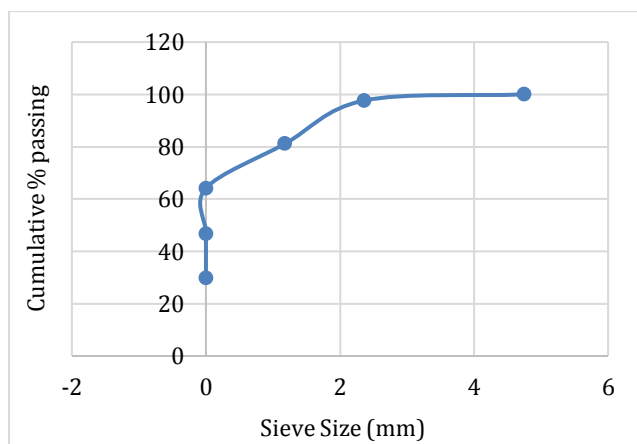


Fig. 3. PSD of QDP (as supplied).

3.1. Properties of QDP

Chemical composition of QDP and PC used for the study (Table 4) shows that the three main oxides (SiO_2 , Al_2O_3 and Fe_2O_3) for QDP which amounted to 88.17% met the requirements of ASTM C618 (2003) for pozzolanic materials. Furthermore, it implies that with the high content of SiO_2 (72.70%) in QDP, it readily reacted with calcium hydroxide (Ca(OH)_2) from the hydration of cement to form additional calcium silicate hydrate (C-S-H) that further enhanced high and early strength gains.

Also, from Table 1, the specific gravity of QDP is less than that of PC and the specific surface area for QDP is higher than that of PC. These properties enhanced high early strength gains as aforementioned. The Loss on ignition (LOI) for QDP and PC conforms to ASTM C 618:2003 provisions.

The particle size distribution (PSD) was carried out on the QDP sample as supplied (Fig. 3) and sieved (Fig. 4).

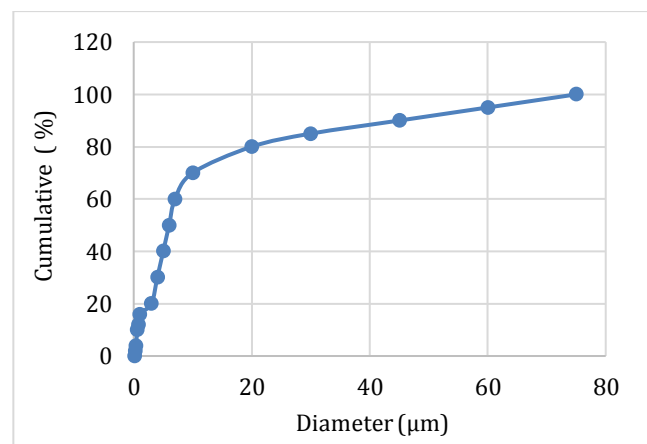


Fig. 4. PSD of sieved QDP.

3.2. Fresh properties of SCC and SCC-QDP

The results of the slump flow, J-ring flow values and blocking ability which measured the filling and passing abilities for all the mixes (SCC, SCC-QD₁₀, SCC-QD₂₀, SCC-QD₃₀ and SCC-QD₄₀) used for the study are shown in Figs 1, 2a&b, and Table 5, respectively. From Fig. 2a and Table 5, slump flow values ranged from 578 mm to 730 mm while the J-ring flow values ranged from 525 mm to 726 mm. The slump flow value and that of the J-ring can be used in combination to assess the passing ability of SCC (ASTM C1621/C1621M, 2008). If the difference between spread diameters ($D_{\text{flow}} - D_{\text{ring}}$) of the two values is less than 25 mm then there is no visible blockage. If it is between 25 and 50 mm then, there is minimal to noticeable blockage. In comparison for both values, the difference is 15 mm, 9 mm and 4 mm for control mix (SCC), SCC-QD₁₀, and SCC-QD₂₀ signifying that these mixes had no visible blocking while for mix SCC-QD₃₀ with a difference of 27 mm flow value exhibited minimal blocking, while for mix SCC-QD₄₀ with a difference of 53 mm flow value exhibited a noticeable blocking (EFNARC, 2005; ASTM C1621/C1621M, 2008)

as shown in Table 5. For all the mixes, no “halo” was observed. Table 5 shows increase in slump flow values for varying concrete mixes while Fig. 5 also show increase in flow values with the replacement of PC with QDP dosage up to 20% when it decreased. This is same for the J-ring flow values. This was enhanced by the high fineness of QDP particles compared with cement particles, which is able to fill the voids between the coarse grains of cement and water molecules which facilitated the flow ability of the mixes. However, beyond 20% replacement of PC with QDP dosage led to excess compared with the quantity required to fill the voids between cement particles and water molecules. These excess particles affected the plastic viscosity of the mix (Rebaye, 2017) which in turn led to a reduction in the slump flow values. The plastic viscosity is a measure of the resistance of SCC to flow due to internal friction. Even though the excess particles caused a reduction in the mix flow ability, it increased resistance to segregation as it helps to thicken the paste, increase in viscosity and density and thus the thickened paste enables the aggregate particles to be uniformly suspended within the SCC paste.

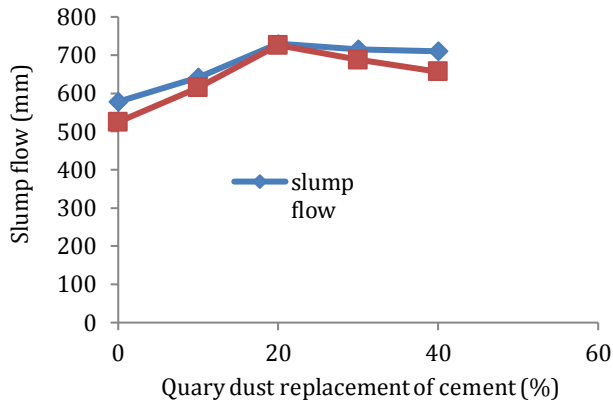


Fig. 5. Slump and J-ring flow values compared.

This shows that all the mixes have good ability, free deformability and the filling and passing abilities met EFNARC-2000 and ASTM C1621/1621M (2006) specifications but for mix SCC-QDP₄₀ that exhibited noticeable blocking. This is not a connected with the fact that SCC-QDP₄₀ has high QDP content leading to high water demand and since water-binder ratio and SP dosage remains constant, led to increase in viscosity. It is interesting to note that with increase in replacement level of PC with QDP content up to 30% slump values were still within Code specifications.

Table 5. Difference between slump flow and J-ring spread diameter.

Mix ID	D_{flow} (mm)	$D_{\text{J-ring}}$ (mm)	$D_{\text{flow}} - D_{\text{J-ring}}$ (mm)
SCC	578	563	15
SCC-QD ₁₀	642	633	9
SCC-QD ₂₀	730	726	4
SCC-QD ₃₀	715	688	27
SCC-QD ₄₀	710	657	53

The results of the blocking ratio (H_2/H_1) shown in Table 6 was to assess the passing ability of the SCC investigated. Nehdi and Landchuk (2003), and Bartos (2005) opined that this blocking ratio is from 0.70 to 0.90 while that of EFNARC, 2005 is from 0.80 to 1.0. Test results showed that all mixes excluding SCC-QD₄₀ met Code specifications. Table 6 shows test results of mixes as regards blocking ratios. The Table shows that SCC-QDP₁₀ and SCC-QDP₂₀ falls under SCC class F1 and F2 for the filling ability in accordance with EFNARC specifications. For the passing ability, the results (Table 6) showed that the aforementioned mixes are in class PA 1 and PA 2, respectively. This means that the mixes exhibited blockage ratio of more than 0.80 which reflects good filling and passing ability; therefore, from the flow and passing ability perspective, all the mixes except SCC-QDP₄₀ met the required criteria for viscosity class 1 to qualify them as SCC in accordance with BS-EN 206-9 (2010).

Table 6. L-box test results.

S/No	Mix ID	H_1 (mm)	H_2 (mm)	H_2/H_1 (mm)
1	SCC	72.80	55.80	0.766
2	SCC-QD ₁₀	72	58.50	0.813
3	SCC-QD ₂₀	71	62.00	0.873
4	SCC-QD ₃₀	73	59.00	0.783
5	SCC-QD ₄₀	79	52.00	0.658

3.3. Hardened Properties

3.3.1. Compressive strength

Fig. 6 shows the compressive strength at varying mixes and also at varying curing ages for the mixes. In figure 8, the compressive strength of concrete for control mix (SCC) compared with that of SCC-QDP₁₀, SCC-QDP₂₀, SCC-QDP₃₀ and SCC-QDP₄₀ at 7 and 14 days are higher because most of the reactions at this stage are attributed mainly to hydration of the PC. Furthermore, in the mixes other than the control, quantity of PC is less which accounts for lower hydration and lower strength. But most importantly, the substitution of PC with pozzolanic materials reduces the initial rate of strength development at early ages due to slow rate of the pozzolanic reaction (Massazza, 1993). At this point in time, the pozzolana (QDP) acts as a filler thus diluting the PC which reduces the strength of the pozzolanic cement compared with that of the control. At later ages the reverse is the case and the pozzolanic cements attains the same or even higher compressive strength than the corresponding control PC. This is because, as the hydration ages, apart from the traditional hydration products from control cement, the QDP reacts with the calcium hydroxide ($\text{Ca}(\text{OH})_2$), a by-product from the PC hydration to form more cementitious materials such as Calcium silicate hydrate (C-S-H) and Calcium -alumina- silicate hydrate (C-A-S-H), leading to an increase in compressive strength of hardened cement pastes and concrete (ACI 232.1R, 1994; Taha et al., 1981). This can be seen in Fig. 6.

The compressive strength of all the mixes increases with curing age as well as with replacement of PC with QDP. As the curing ages, hydration continued and more hydration products are formed especially after 28 days when hydration products or cementitious materials which came from PC and the reaction between $\text{Ca}(\text{OH})_2$ and QDP which accounts for the increase in strength. This is not unconnected with the fact that the hydration product possessed a large specific volume than the unhydrated cement particle leading to the accumulation and compaction of these hydrated products which gave rise to higher strength. The compressive strength values of the mixes increased with age and varying replacement of PC with QDP up to 20% then decreased. The increase in compressive strength is due to the pozzolanic reaction between $\text{Ca}(\text{OH})_2$ and the silica content of QDP as aforementioned as well as hydration of the silica content of QDP (Yu et al., 1999). The decrease in compressive strength beyond 20% replacement

of PC with QDP may be due to the fact that the quantity of QDP present in the mix is higher than the amount required to react with the liberated $\text{Ca}(\text{OH})_2$ during the hydration process leading to presence of excess silica leaching out and causing a deficiency in strength as evident in the work of Al-Khalaf and Yousif (1984). Furthermore, the depletion of $\text{Ca}(\text{OH})_2$ in the mix solution probably lowered the PH of the pore water in the mix solution thereby leading to decrease in strength (Maragu et al., 2018). This can also be attributed to the fact that the W/B ratio remains constant and with increase in silica content requires more water and $\text{Ca}(\text{OH})_2$ for more reaction to produce more C-S-H and C-A-S-H but are not available, because subsequent reactions has stabilized these ions. This dis-stabilizes the system leading to decrease in strength. It is of interest to note that QDP has high specific surface area that requires more water, hence 20% content of QDP can be considered as optimum limit for the replacement of PC.

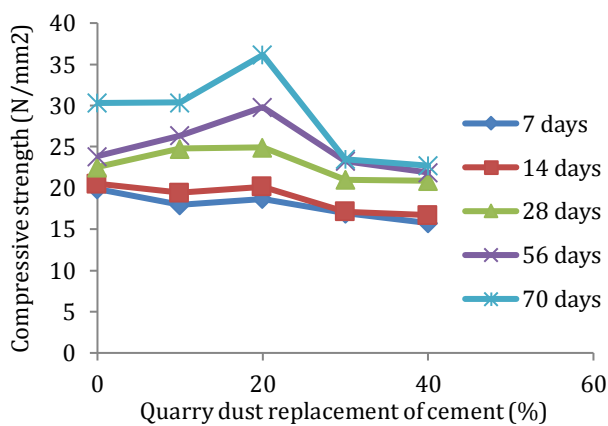


Fig. 6. Compressive strength for varying mixes at varying ages.

3.3.2. Splitting tensile strength

Fig. 8 shows the results of splitting tensile test (Fig. 7) conducted on cylindrical concrete specimens. For control and pozzolanic cement mixes, strength increases with curing ages as expected. This is because splitting tensile strength is related to compressive strength. For the control specimens, there is an increase of 5.52 in 28 days from 7 days and 9.68% in 70 days. Maximum strength increase of about 22.41% was obtained for mix SCC-QDP₂₀ at 70 days from 7 days and a minimum increase in strength of 16.89% for mix SCC-QDP₄₀ for the same period. This shows that split tensile strength of SCC is influenced by the replacement of PC with QDP content.

4. Conclusions

To gain a compressive understanding of the influence of QDP replacement of cement in SCC, performance in terms of optimum use of QDP as a replacement of cement, fresh and mechanical properties of five mixtures of SCC containing QDP at varying levels (0, 10, 20, 30, and 40) of cement replacement were evaluated. From the results, discussion and findings from the study, the following conclusion can be drawn:



Fig. 7. Splitting tensile testing.

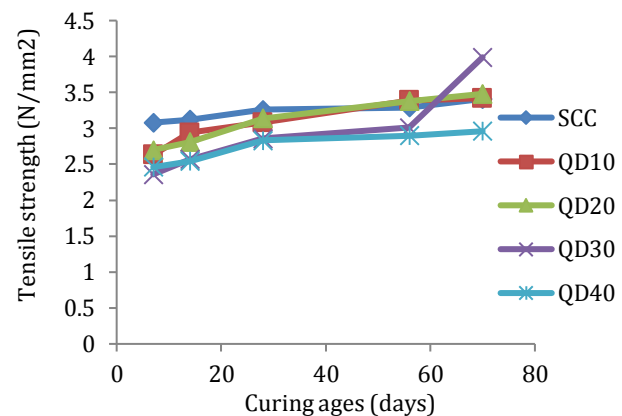


Fig. 8. Splitting tensile test results.

- Substitution of PC with QDP in SCC mixes positively improves its fresh properties as evident in slump/J-ringing flow values, filling and passing ability values which meets EFNARC, 2005 specifications.
- Quarry dust particles can be used to replace PC in SCC up to 20% optimum without any adverse effect on its properties.
- The replacement of PC with QDP higher than 20% by mass of PC led to reduction in both physical and mechanical properties.
- In the production of SCC mixtures the use of QDP extend its technical and environmental benefit since it reduces air pollution and health hazards resulting from its production at sites and disposal. However, its use beyond 20% replacement of PC in SCC has adverse effects on both physical and mechanical properties and requires higher dosage of Super plasticizer to achieve similar properties which is an addition to cost of production.

The research mainly evaluated the fresh and mechanical properties of SCC containing QDP at a fixed W/B and SP content. Further comprehensive studies are required to investigate the hydration behavior, micro structure and durability properties of SCC containing QDP at more than 20 % content, varying W/B and super plasticizer contents.

REFERENCES

- ACI 232.1R (1994). Use of natural pozzolans in concrete. American Concrete Institute, Farmington Hills, MI, U.S.A.
- Al-Khalaf MN, Yousif HA (1984). Use of rice husk ash in concrete. *International Journal of Cement Composites and Lightweight Concrete*, 6(4), 241–248.
- Allam ME, Bakhoum ES, Garas GI (2016). Re-use of granite sludge in producing green concrete. *ARPJ Journal of Engineering and Applied Sciences*, 9, 2731–2737.
- Al-Rubaye MMK (2016). Self-compacting Concrete: Design, Properties and Simulation Flow Characteristics in the L-Box. *Ph.D thesis*, Cardiff University, UK.
- ASTM C1621/C1621M (2006). Standard test method for passing ability of self-compacting concrete by J – Ring. ASTM International, West Conshohocken, P.A., U.S.A.
- ASTM C494 (2004). Standard specification for chemical admixtures for concrete. ASTM International, West Conshohocken, P.A., U.S.A.
- ASTM C496/C496M (2004). Standard test method for splitting tensile strength of cylindrical concrete specimens. ASTM International, West Conshohocken, P.A., U.S.A.
- ASTM C618 (2003). Specification for coal fly ash and raw of calcined material pozzolan for use in concrete. ASTM International, West Conshohocken, P.A., U.S.A.
- ASTM C642 (2013). Standard test method for density, absorption, and voids in hardened concrete. ASTM International, West Conshohocken, P.A., U.S.A.
- Baboo R, Khan NH, Abuwshek RS, Tabui RS, Duggal SK (2011). Influence of marble powder/granules in concrete mix. *International Journal of Civil Engineering and Technology*, 4, 827–834.
- Bartos PJM (2005). Testing – SCC: Towards new European standards for fresh SCC. *First international symposium on design performance and use of self-consolidating concrete*, Changsha, Hunan, China.
- Belaidi AE, Azzouz L, Kadi I, Renai S (2012). Effect of natural pozzolana and marble powder on the properties of self-compacting concrete. *Construction and Building Materials*, 31, 251–257.
- BS EN 12350-2 (2009). Testing fresh concrete, slump test. British Standards Institution, London, England.
- BS EN 12390-3 (2009). Testing hardened concrete; compressive strength of test specimens. British Standards Institution, London, England.
- BS EN 196-6 (1997). Method of testing cement, determination of fineness. British Standards Institution, London, England.
- EFNARC (2005). Specifications and Guidelines for self-compacting concrete. European Association for Producers and Applicators of Specialist Building Products, UK.
- EFNARC (2005). The European Guidelines for self-compacting concrete: Specification, production and use. European Association for Producers and Applicators of Specialist Building Products, UK.
- Gowda MR, Naragimhan MC, Kaniddappa RGV (2000). Study of properties of SCC with Quarry dust. *Indian Concrete Journal*, 83(8), 54–60.
- Hafez E, Elyamany AM, Abdelmoaty, Basma M (2014). Effect of filler types on physical, mechanical and microstructure of self-compacting concrete and flow able concrete. *Alexandria Engineering Journal*, 53, 295–307.
- Ho DWS, Shein AMM, Ng CC, Tam CT (2002). The use of quarry dust for SCC Applications. *Cement and Concrete Research*, 32, 505–511.
- Kumar NVS, Rao PB, Sai MLNK (2013). Experimental study on partial replacement of cement with quarry dust. *International Journal of Advanced Engineering Research Studies*, 3, 136–137.
- Manju P et al. (2014). Feasibility and Need for Use of Waste Marble Powder in Concrete Production. 2349-943435, 1-6.
- Manju R, Premalatha J (2016). Binary, ternary and quaternary effect of pozzolanic binders and filler materials on the properties of self-compacting concrete. *International Journal of Advanced Engineering Technology*, 5(2), 674–683.
- Maragu JM, Thiong'O JK, Wachira JM (2018). Chloride ingress in chemically activated calcined clay based cement. *Journal of Chemistry*, 2018, 1595230, 1–8.
- Massazza F (1993). Pozzolanic cements. *Cement and Concrete Composites*, 75(4), 185–214.
- Ouchi M, Nakamura S, Osterson T, Hellberg S, Iwin M (2003). Applications of self-compacting concrete in Japan. ISHPC, Europe and the United States, 1–20.
- Poo CE, Ho DWA (2004). Feasibility study on the utilization of r-FA in SCC. *Cement and Concrete Research*, 34(12), 2337–2339.
- Poppe AM, Schutter GD (2005). Cement hydration in the presence of high filler contents. *Cement and Concrete Research*, 35(12), 2290–2299.
- Rizwan SA, Bier TA (2012). Blends of Limestone powder and fly ash enhance the response of self-compacting mortars. *Construction and Building Materials*, 27, 398–403.
- Sahmaran M, Christianto HA, Yaman IO (2006). The effect of chemical admixtures and mineral additives on the properties of self-compacting mortars. *Cement and Concrete Composites*, 28(5), 432–440.
- Sumer P (2016). Use of granite waste as powder in SCC. *International Research Journal of Engineering and Technology (IJRET)*, 3(6), 1129–1135.
- Uysal M, Sumer M (2011). Performance of self-compacting concrete containing different mineral admixtures. *Construction and Building Materials*, 25, 4112–4120.
- Uysal M, Yilmaz K (2011). Effect of mineral admixtures on properties of self-compacting concrete. *Cement and Concrete Composites*, 33, 771–776.
- Vijayalakshimi M, Sekar AS, Prabhu GG (2013). Strength and durability properties of concrete made with granite Industry waste. *Construction and Building Materials*, 46, 1–4.
- Wenzhong Z, Gibbs JC (2005). Use of different limestone and Chalk powders in Self-Compacting concrete. *Concrete Research*, 35, 457–462.
- Ye G, Liu X, De Scutter GD (2007). Influence of limestone powder used as filler in SCC on hydration and microstructure of cement pastes. *Cement and Concrete Composites*, 29(2), 94–102.



Research Article

Effect of nano silica on cement mortars containing micro silica

İlknur Bekem Kara^{a,*} , Ömer Furkan Durmuş^b 

^a Department of Construction Technology, Borçka Acarlar Vocational School, Artvin Çoruh University, Artvin, Turkey

^b Karadeniz Technical University Faculty of Engineering, Department of Civil Engineering, Trabzon, Turkey

ABSTRACT

The use of cement and concrete is becoming increasingly widespread all over the world. However, the high energy consumption required for the production of clinker and the greenhouse gas emissions generated during production negatively affect both the economy and the environment. In the studies conducted for many years, researchers have found that the substitution of various pozzolans with cement provides both technical advantages and environmental benefits. The use of pozzolans in cementitious composites provides advantages such as the improvement of the physical and mechanical properties of the material, the conservation of the environment and the economy in terms of the evaluation of industrial wastes. In recent years, studies on the use of nanoparticles in cementitious composites are positively. In this study, it was aimed to investigate the properties of fresh and hardened cement mortars using micro silica as pozzolan and nano silica as nanoparticle. For this purpose, four different cement pastes and mortars mixtures were prepared by substituting 0%, 1%, 2%, 3% nano SiO₂ (silica) cement in mortar mixtures containing 5% micro silica. The effects of the nano silica on the micro silica-containing cement paste on the consistency and setting time were investigated. The mortar mixtures produced were subjected to flexural and compressive strength tests on days 7, 28 and 90th. SEM images of mortar mixtures were taken. As a result, it was found that 2% nano silica admixture of 5% micro silica containing cement admixture affects the flexural and compressive strength positively, whereas 2% nano silica admixture increased the flexural strength by 13% and compressive strength by 7%.

ARTICLE INFO

Article history:

Received 17 May 2019

Revised 15 June 2019

Accepted 26 June 2019

Keywords:

Mortar

Micro silica

Nano silica

Strength

1. Introduction

In the World, studies for discovering new areas with respect to nano technologies applications in all science and engineering branches have gone on. In construction sector, researches on using carbon nano tubes and nano particles in concrete, ceramics and glass production have been made. Specifically in cement based composites, strength and durability enhancing through nano material usage is at the top ranks among expected returns (Özbora et al., 2013; Bozoğlu and Arditi, 2012). Additionally, today scientists doing research about nano technology in concrete and cement concentrate on hydration reaction and effects of nano particles over concrete features (Özbora et al., 2013).

Concrete is a composite material and includes hydration products in nano and micro scale. Particle sizes and specific surface areas of concrete constituents are seen in Fig. 1. Although it is resulting from the Fig. 1 that conventional concrete doesn't contain nano particle, chemical additives, water in gel spaces and as a hydration product C-S-H gels are indeed nano scale substances.

In concrete sector, researches for nano technology usage is going on but, it is known that applications are limited. However, improvement of physical and mechanical characteristics in cement-based materials are certain according to obtained results. Some developments obtained in cement-based composites through nano particles usage are summarized below (Özbora et al., 2013):

* Corresponding author. Tel.: +90-506-628-9627 ; Fax: +90-466-215-1072 ; E-mail address: ilknurbekem@artvin.edu.tr (İ. Bekem Kara)
ISSN: 2548-0928 / DOI: <https://doi.org/10.20528/cjcr.2019.02.003>

- Adherence between aggregate and cement paste strengthens.
- Micro crack generation decreases, and these cracks heals by their self.
- Concrete permeability declines.
- Shrinkage generation diminishes.
- Negative effect of aggregates involving clay lessen.
- Elasticity module increases.
- Resistance of concrete to heat rises.
- Durability features like alcali silica reaction, corrosion, freezing-dissolution improve.

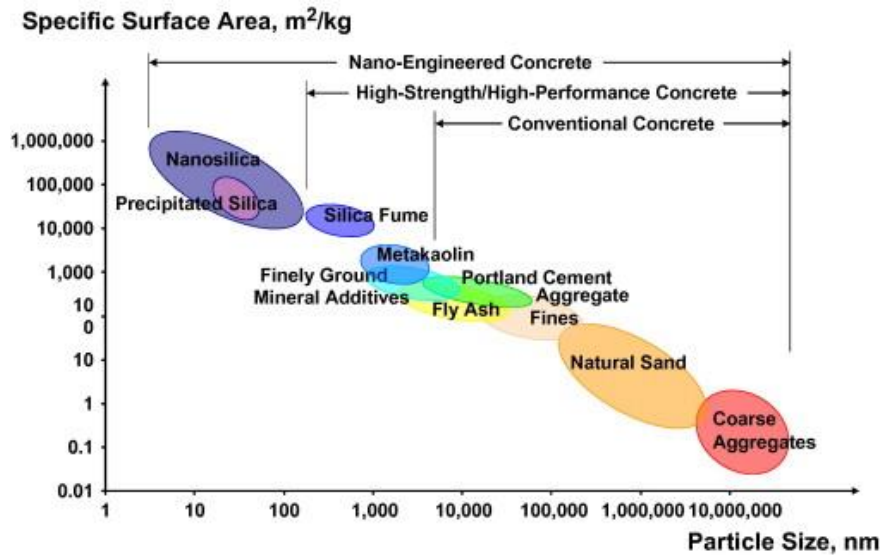


Fig. 1. Particle sizes and specific surface areas of concrete materials.

The most commonly used nano particles in cement and concrete are nano SiO_2 , nano Al_2O_3 and nano TiO_2 . Studies about nano particle usage over hydration, rheological structure, micro pattern, strength, elasticity module features of cement and concrete have been in literature. Some results of these studies are:

- Compressive strength of cement mortar increases 111.2% on 7th day and 108.6% on 28th day via adding 1% nano CaCO_3 to cement mortar by weight, while compressive strength of concrete mortar rises 14% on 7th day and 16.7% on 28th day via adding 1% nano Al_2O_3 to concrete mortar by weight (Zhang et al., 2015).
- When water/cement ratio is 0.40 and 0.60, the highest compressive strength in both water/cement ratios on 28th day is given by mortars involving 5% nano TiO_2 among 0%, 1%, 3% and 5% of TiO_2 usage ratios (Lee et al., 2013).
- In a study about self-compacting concrete that is blended with nano SiO_2 and fly ash, the highest compressive strength on 28th day is in self compacting concrete samples containing 0% fly ash and 4% nano SiO_2 (Güneyisi et al., 2015).
- According to another study that nano SiO_2 , $\text{Cu}_{0.5}\text{Zn}_{0.5}\text{Fe}_2\text{O}_3$ ve NiFe_2O_4 powders are used, optimum dosage is 3% in concretes produced with nano SiO_2 , while it is 2% in the other concretes using $\text{Cu}_{0.5}\text{Zn}_{0.5}\text{Fe}_2\text{O}_3$ and NiFe_2O_4 powders. Concrete samples involving nano SiO_2 give better results than samples containing $\text{Cu}_{0.5}\text{Zn}_{0.5}\text{Fe}_2\text{O}_3$ and NiFe_2O_4 (Amin and Abu El-Hassan, 2015).

Pozzolana usage is commonly used in cement-based composites. Through adding silica fume to concrete,

compressive strength increases, shrinkage decreases, abrasion resistance rises, adherence grows and permeability diminishes. Economical and ecological benefits of silica fume should not be overlooked in addition to its positive contribution over concrete features (Topçu and Canbaz, 2002). It is well known that the addition of micro silica can improve the strength and durability of concrete and the addition of nano silica can also improve certain properties of concrete (Li et al., 2017). In literature context, micro and nano silica usage in both cement mortars and concrete is seen to be extensive.

The aim of this study is to determine usability of 2 materials that have micro and nano sizes together in cement mortars. Silica fume and nano silica are preferred respectively as a micro material and nano particle. Moreover, nano silica's effects over mechanical characteristics of silica fume added cement mortars are investigated.

2. Materials and Method

2.1. Materials

In the study, the CEM I 42,5 R cement supplied from Akcansa Cement Plant, micro silica, nano silica, CEN standard sand and mains water are used. Chemical, physical and mechanical properties of the cement are given in the Table 1 (TS EN 197-1 2012).

Micro silica that has a 2.32 g/cm³ particle density is supplied from Antalya Eti Electro-Metallurgy Plant. Its chemical features are seen in the Table 2.

Table 1. Chemical, physical and mechanical properties of the CEM I 42,5 R cement.

Analysis	Oxide	Value	Analysis	Tests	Value
Chemical (%)	CaO	62.64	Physical	Blaine, cm ² /g	3269
	Al ₂ O ₃	4.56		Volume expansion, mm	2.0
	Fe ₂ O ₃	3.36		Intensity, g/cm ³	3.12
	SiO ₂	19.05		Setting start time, min.	150
	SO ₃	2.88		Setting finish time, min.	210
	MgO	2.98	Mechanical	Day	MPa
	Na ₂ O	0.15		2. day	32.5
	Ignition loss	3.02		7. day	43.4
	Insoluble residue	0.30		28. day	53.6

Table 2. Micro silica's chemical features.

Oxide	SiO ₂	Al ₂ O ₃	Fe ₂ O ₃	CaO	MgO	SO ₃
Micro silica	81.40	4.47	1.40	0.82	1.48	1.30

Nano silica's average particle size is 30 nm and has a 99.9% purity. B.E.T. surface area is 440 m²/g, its color is white. Nodular nano SiO₂ has a density between 2.2-2.6 g/m³. Binding materials used during the study are seen in the Fig. 2.

CEN standard sand in conformity with TS EN 196-1 supplied from Kırklareli Limak Cement Plant is used in mortar admixtures. Its sieve analysis is given the Table 3.

In the study, cement pastes and mortar admixtures are produced in four different groups and defining codes are given to the samples. The codes are shown in the Table 4.

On the prepared cement pastes, consistency experiments and determination tests for initial and final setting time are done according to the TS EN 196-3.

According to the TS EN 196-1 mass ratios of mortar constituents are prepared in the way of 1 portion cement (450 gr), 3 portions standard sand and 0,5 portion water (225 gr). In this study, 4 different mortar admixtures are prepared with cement, micro silica, nano silica, standard sand and water. Material quantities for the mortar admixtures are seen in the Table 5.

Samples belonging to the mortar admixtures 5S, 5S+1NS, 5S+2NS and 5S+3NS are subjected to flexural strength test on 7th, 28th, 90th days. The experiment carried out with 3-point method. Prismatic samples that have 40 mm x 40 mm x 160 mm sizes (TS EN 196-1, 2016).

**Fig. 2.** a) Micro silica; b) Nano silica; c) Cement.**Table 3.** Standard sand sieve analysis.

Square aperture size (mm)	Cumulative retaining at sieve (%)
2.00	0
1.60	7±5
1.00	33±5
0.50	67±5
0.16	87±5
0.08	99±1
0.00	0

Table 4. Codes of the mortar samples.

Sample Name	Code
Cement pastes or mortar with 5% micro silica substitution	5S
Cement pastes or mortar with 5% micro silica + 1% nano silica substitution	5S+1NS
Cement pastes or mortar with 5% micro silica + 2% nano silica substitution	5S+2NS
Cement pastes or mortar with 5% micro silica + 3% nano silica substitution	5S+3NS

Table 5. Material quantities for the mortar admixtures.

Sample Code	Cement, gr	Micro silica, gr	Nano silica, gr	Standard sand, gr	Water, gr
5S	427.5	22.5	0	1350	255
5S+1NS	423.0	22.5	4.5	1350	255
5S+2NS	418.5	22.5	9.0	1350	255
5S+3NS	414.0	22.5	13.5	1350	255

Compressive strength experiments are made on the 6 samples with 40 mm x 40 mm x 40 mm size resulting from flexural strength. Compressive strength device is arranged at appropriate capacity and loading speed (2400 ± 200) N/s for the experiment. Semi-prisms obtained after flexural test are located without overflowing not more than ± 5 mm between plates of the device by centering. Loading to the device are made until it is cut at (2400 ± 200) N/s speed. The result of compressive strength experiment are stated as arithmetical mean of 6 results that are assigned from 3 prism sets (TS EN 196-1, 2016).

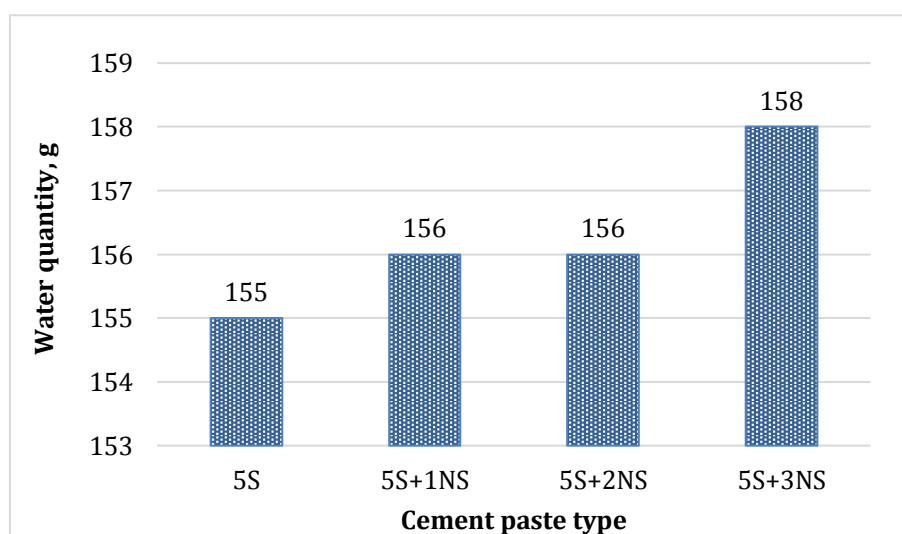
3. Results and Discussion

In the study, by being put in nano silica substitution in the ratios respectively 0%, 1%, 2% and 3% to the 5% mi-

cro silica added cement pastes and mortar samples, admixtures are prepared. Consistency- setting time determination tests are made on cement pastes belonging to 5S, 5S+1NS, 5S+2NS and 5S+3NS admixture, whereas on mortars, compressive- flexural experiments are done on 7th, 28th and 90th days.

The results obtained from the consistency test over the cement pastes with micro silica (5%) and nano silica (0%, 1%, 2%, and 3%) substitution are seen in the Fig. 3. Nano silica substitution slightly effects water necessity. Water quantity increased by 0.65% for 1% and 2% substitution rates according to the 5% micro silica substitution (0% nano silica substitution). 3% nano silica substitution increased the water requirement by 3%.

The results obtained from setting time experiments over the 5% micro silica and nano silica substituted (with different rates) cement pastes are seen in the Fig. 4.

**Fig. 3.** Water necessities of cement pastes with micro and nano silica substitutions.

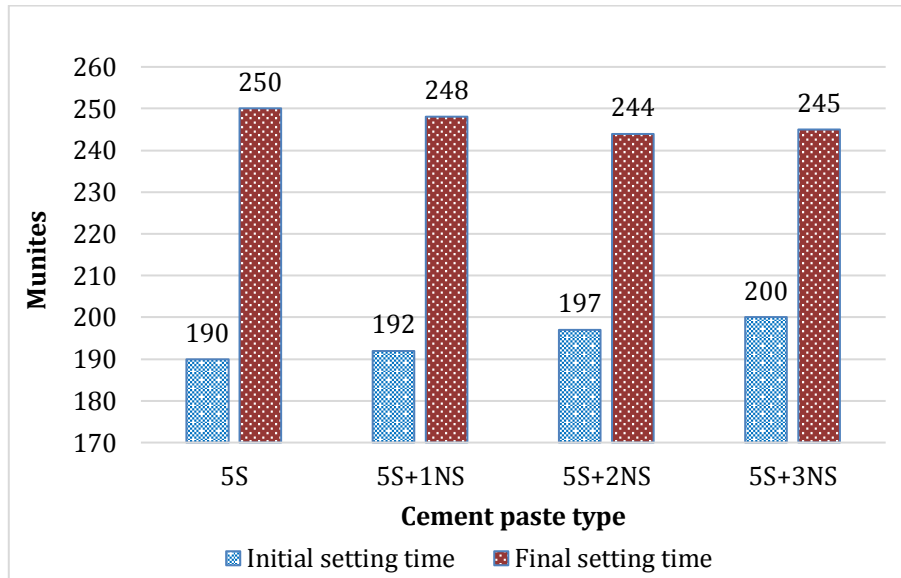


Fig. 4. Initial and final setting times of cement pastes with micro and nano silica substitutions.

When initial and final setting times of the 5S, 5S+1NS, 5S+2NS and 5S+3NS cement pastes are analyzed, it is seen that initial setting time extends whereas final setting time decreases in condition that nano silica substitution increases. Cement mortar containing 5% micro and 3% nano silica have more initial setting time. 3% nano silica substitution increases initial setting time by 5% compare to cement paste without nano silica. This result is parallel with literature. Kumar and Singh (2018) studied the effect of nano silica on setting times and observed that initial setting time increases with the addition of nano silica (Kumar and Singh, 2018).

Cement technology and industry that developed fast in the end of 19th century has gradually shown progress from the point of quality. Cement enters the hardening (setting) process by starting reaction when it gets in touch with water. This process stays in certain limits. Standards define at least 1 hour and 10 hours respectively for setting starting and setting finishing time. If setting starting process is fast, carrying and placing of fresh concrete is very difficult. If hardening becomes late,

concrete can't obtain its strength in desired time and formwork removal time lingers. So, concrete is affected from out climate conditions (Çelik et al., 2004).

Cement pastes belonging to mixtures that produced in study progress, don't exceed the rule "initial setting time can't be less than 1 hour" defined in the standard (TS EN 197-1, 2012).

Çelik et al. (2001), researched silica fume's effect over Portland cement's setting time through 5%, 10% and 15% silica fume substituted to Portland cement and found that the mixture with 5% silica fume had no effect to setting time while the mixtures with 10% and 15% silica fume clearly delays setting times.

Findings obtained from flexural strength tests over the 5% micro silica and nano silica substituted (with different rates) mortar samples that were done on 7th, 28th and 90th days are given in the Fig. 5.

Changes of flexural strengths when substituting nano silica to micro silica added mortars are concluded at the Table 6. At all ages, the best flexural strength value belongs to 5S+2NS mortar admixtures.

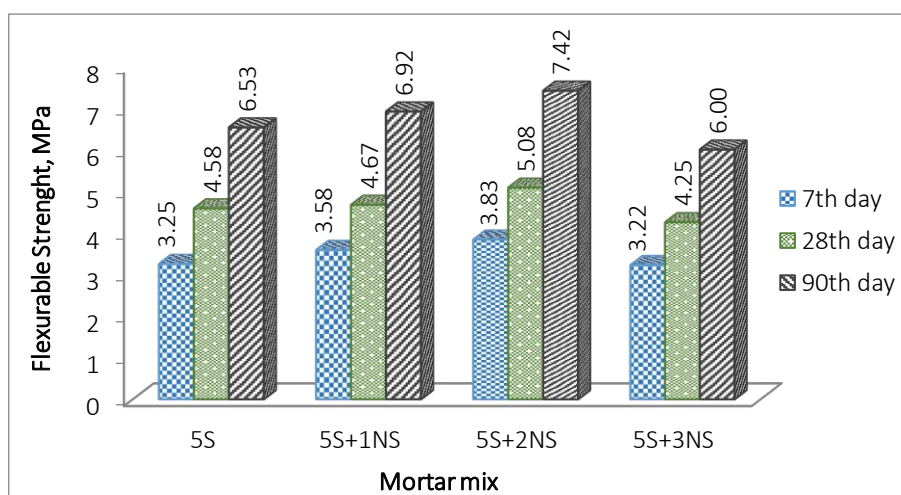


Fig. 5. Flexural strength results of mortar mixtures.

Table 6. According to 5% micro silica added mortars, the effect of nano silica substitution over flexural strength (+, increases; -, decreases).

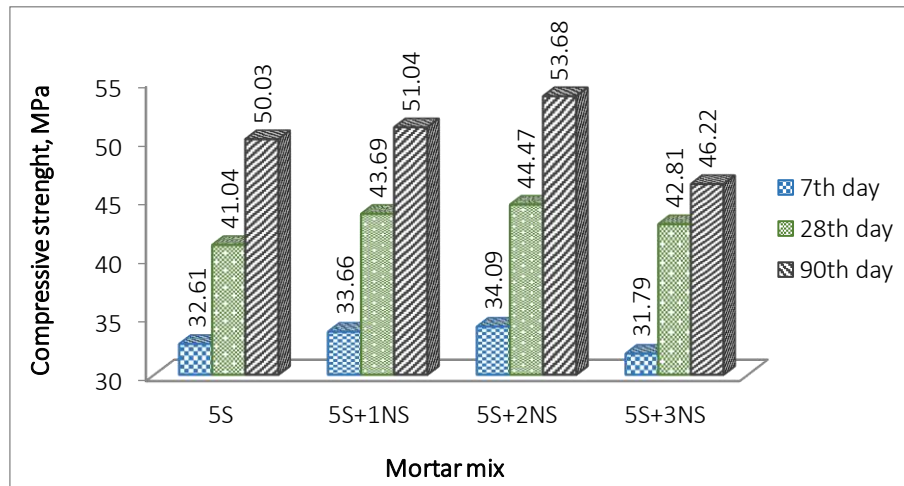
Substitution Rate	7 th day	28 th day	90 th day
%1 NS	+10.0	+2.0	+6.0
%2 NS	+17.0	+10.0	+13.0
%3 NS	-1.0	-7.0	-8.0

Among the mortar samples whose flexural strength studied, the highest strength values on 7th, 28th and 90th days are obtained from 5S+2NS mortar mixtures. According to 5% micro silica added mortars 1% and 2% nano silica substitution increases flexural strength respectively 6% and 13% on 90th day, while 3% nano silica substitution decreases flexural strength.

Findings obtained from compressive strength tests over the 5% micro silica and nano silica substituted

(with different rates) mortar samples that were done on 7th, 28th and 90th days are given in the Fig. 6.

Changes of compressive strengths when substituting nano silica to micro silica added mortars are concluded at the Table 7. At all ages, the best compressive strength value belongs to 5S+2NS mortar admixtures. On 90th day, 2% nano silica substitution increases compressive strength 7%.

**Fig. 6.** Compressive strength results of mortar mixtures.**Table 7.** According to 5% micro silica added mortars, the effect of nano silica substitution over compressive strength (+, increases; -, decreases).

Substitution Rate	7 th day	28 th day	90 th day
%1 NS	+3.0	+6.5	+2.0
%2 NS	+4.5	+8.0	+7.0
%3 NS	-2.5	+4.0	-7.5

Li et al. (2017) determined micro and nano silica using increases cube strength, sulphate, carbonation and chlorine resistance. However, it is found that based on powder type and combination, nano powders usage in mortars containing micro silica has an upper limit. In a study, this limit is specified as 1.25% and it is ascertained that when it is surpassed, quantity of space grow because of coagulation (Oltulu and Şahin, 2013). In this study, it is found nano silica usage with a ratio of 3%, decreases both flexural and compressive strength. In this context, it is thought that coagulation happened with a 3% ratio and due to the spaces, this coagulation affects strengths negatively.

Jo et al. 2007 explored that in nano SiO₂ is a filler material developing microstructure and the more silica fume and nano SiO₂ quantities increase, the more compressive strength of mortar increases (7th and 28th day). Also it is known that the compressive and flexural strength of the cement mortars with nano SiO₂ were higher than that of the plain cement mortar (Li et al., 2004).

The authors (Haruehansapong et al., 2014) investigated on the cement composite with silica fume and with 9% of nano SiO₂. It was found that the microstructure of control cement paste and cement paste with silica fume was similar. The silica fume has lesser pozzolanic activity and filling ability compared to nano SiO₂.

Li et al. (2018) demonstrated that with both micro silica and nano SiO₂ added together, the compressive strength and elastic modulus could be increased to higher than those achievable with only MS added or only NS added.

SEM images obtained from the mortar samples 5S, 5S+1NS, 5S+2NS and 5S+3NS are seen in the Fig. 7. According to the SEM images of all the cement mortars, C-S-H phase which is intensively prevalent to the structure is seen. Formless gel constitutes prevalent phase in the all structure, forms a linkage between hydration products and tries to fill spaces. The phase tries to fill the spaces in the 5S cement paste, but the 1-2 micron length sporadic spaces are encountered even though they are

very few. Additionally, cracks are run across even if they have very small sizes.

Besides, it is seen that 5S+1NS and 5S+2NS coded cement pastes have a more solid and stable structure. Abd El-Baky et al. (2013) determined that cement mortar containing nano silica have more homogeneity binder, less pores, more adhesion at interfacial zone in SEM analysis. However, it is found that as per the other samples, 5S+3NS cement paste has a more porous structure that is up to 3 micrometer. It is known that excessive dosage of NS would result in more serious agglomeration of nano particles, with decline in nano effect (Zhanga et al., 2018).

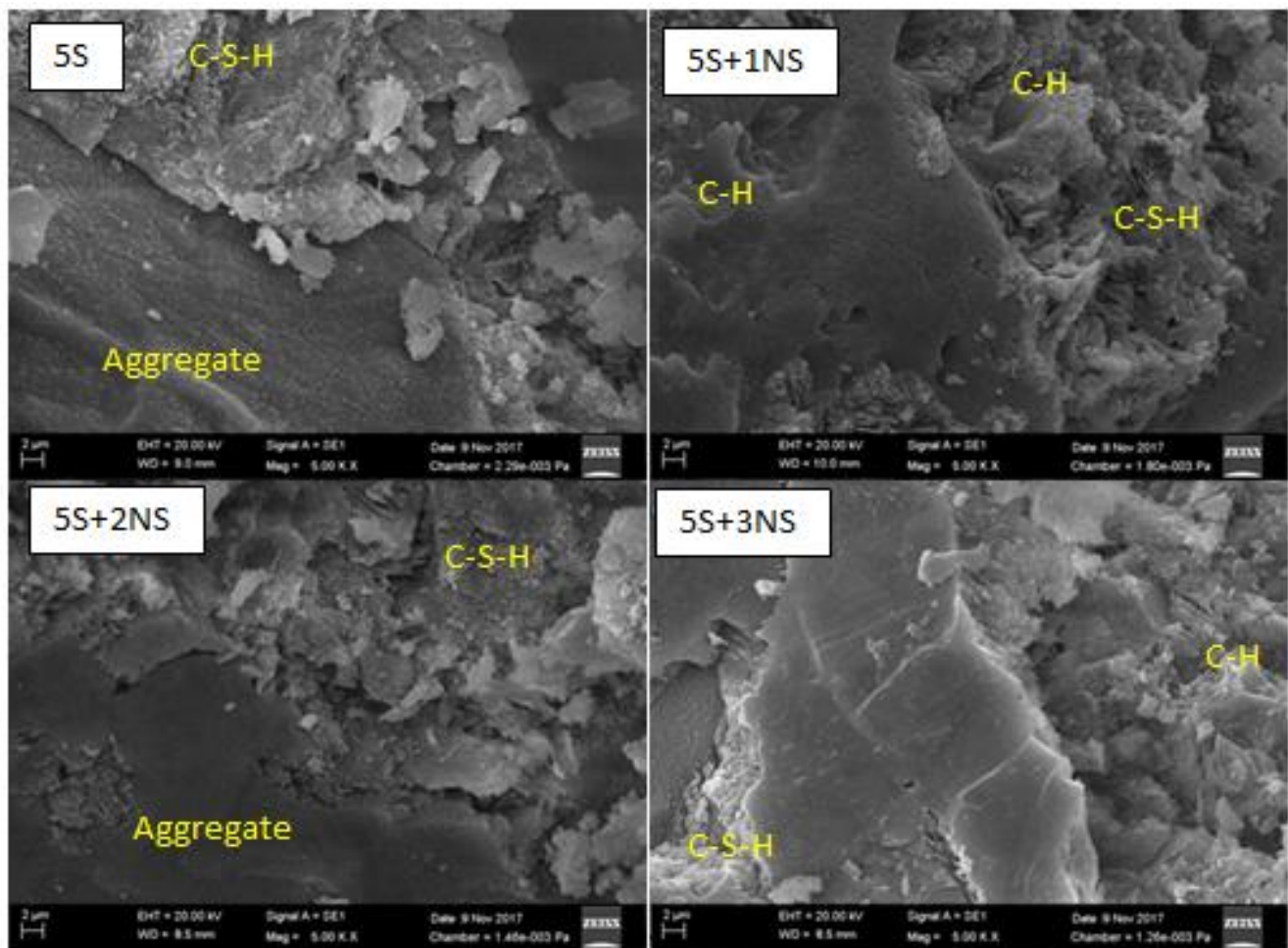


Fig. 7. SEM images of the mortar admixtures.

4. Conclusions

According to consistency, initial and final setting time experiments over the cement pastes of 5S, 5S+1NS, 5S+2NS and 5S+3NS mixtures, it is found that 3% nano silica substitution somewhat increases water necessity and all the nano silica substitutions extend initial setting time whereas they shorten final setting time as per mortar mixture containing 5% micro silica.

With regard to flexural and compressive strength tests on 7th, 28th and 90th days over the cement pastes of 5S, 5S+1NS, 5S+2NS and 5S+3NS mixtures, in comparison with mortar samples containing 5% micro silica, it is

detected 1% and 2% nano silica substitutions increases flexural and compressive strength, whereas 3% nano silica substitution decreases these strengths.

It is established that 2% nano silica substitution to 5% micro silica added cement mortars affects flexural and compressive strength positively. On 90th day, 2% nano silica substitution increases flexural strength 13% and compressive strength 7%.

On the other hand, 3% nano silica substitution decreases 8% flexural strength and compressive strength 7.5% in comparison with mortar mixture containing 5% micro silica.

Acknowledgements

This research has been supported via 2016.F94.02.02 numbered Project by Artvin Çoruh University Scientific Research Projects Fund. The authors gratefully acknowledge the financial support provided by Artvin Çoruh University.

Publication Note

This research has previously been presented at International Civil Engineering and Architecture Conference (ICEARC'19) held in Trabzon, Turkey, April 17-20, 2019. Extended version of the research has been submitted to Challenge Journal of Concrete Research Letters and has been peer-reviewed prior to the publication.

REFERENCES

- Abd El-Baky S, Yehia S, Khalil IS (2013). Influence of nano-silica addition on properties of fresh and hardened cement mortar. *NANOCON Brno*, Czech Republic, EU, 10, 16–18.
- Amin M, Abu el-hassan K (2015). Effect of using different types of nano materials on mechanical properties of high strength concrete. *Construction and Building Materials*, 80, 116–124.
- Bozoğlu Demirdöven J, Arditi D (2012). Nanotechnology applications in structures and construction management. 2. *Project and Construction Management Congress*, İzmir, Turkey, 43.
- Çelik MH, Özgan E, Kösen N (2004). The Effect of crom magnesit brick dust on the starting and finishing setting time of portland cement. *Journal of Polytechnic*, 7(1), 79–85.
- Çelik MH, Şimşek O, Sancak E (2001). The Effect of silica fume on the starting and finishing setting time of portland cement. *Journal of Polytechnic*, 4(4), 55–60.
- Güneyisi E, Gesoğlu M, Al-Goody A, İpek S (2015). Fresh and rheological behaviour of nano-silica and fly ash blended self-compacting concrete. *Construction and Building Materials*, 95, 29–44.
- Haruehansapong S, Pulngern T, Chucheeepsakul S (2014). Effect of the particle size of nanosilica on the compressive strength and the optimum replacement content of cement mortar containing nano-SiO₂. *Construction and Building Materials*, 50, 471–477.
- Jo B, Kim C, Tae G, Park J (2007). Characteristics of cement mortar with nano-SiO₂ particles. *Construction and Building Materials*, 21, 1351–1355.
- Kumar A, Singh G (2018) Effect of nano silica on the fresh and hardened properties of cement mortar. *International Journal of Applied Engineering Research*, 13, 11183–11188.
- Lee BY, Amal R, Jayapalan AR, Kurtis KE (2013). Effects of nano-TiO₂ on properties of cement-based materials. *Magazine of Concrete Research*, 65(21), 1293–1302.
- Li H, Xiao H, Yuan J, Ou, J (2004). Microstructure of cement mortar with nano-particles. *Composites: Part B*, 35, 185–189.
- Li LG, Zheng JY, Zhu J, Kwan AKH (2018). Combined usage of micro-silica and nano-silica in concrete: SP demand, cementing efficiencies and synergistic effect. *Construction and Building Materials*, 168, 622–632.
- Li LG, Zhu J, Huang ZH, Kwan AKH, Li LJ (2017). Combined effects of micro-silica and nano-silica on durability of mortar. *Construction and Building Materials*, 157, 337–347.
- Oltulu M, Şahin R (2013). Effect of Nano-SiO₂, nano-Al₂O₃ and nano-Fe₂O₃ powders on physico-mechanical properties of cement mortar containing silica fume. *Ready Mixed Concrete Congress*, İstanbul, Turkey, 225–235.
- Özbora AA, Tarhan M, Engin Y (2013). The Role of nanotechnology in the future of concrete. *Ready Mixed Concrete Congress*, İstanbul, Turkey, 304–312.
- Sanchez F, Sobolev K (2010). Nanotechnology in concrete-a review. *Construction and Building Materials*, 24, 2060–2071.
- Topçu İB, Canbaz M (2002). Investigation of the interfacial surfaces of concrete with silica fume. *ECAS 2002 International Building and Earthquake Engineering Symposium*, Ankara, Turkey, 469–476.
- TS EN 196-1 (2016). Methods of testing cement-Part 1: Determination of strength. Turkish Standards Institution, Ankara, Turkey.
- TS EN 196-3 (2016). Methods of testing cement -Part 3: Determination of setting times and soundness, Turkish Standards Institution, Ankara, Turkey.
- TS EN 197-1 (2012). Cement-Part 1: Composition, specification and conformity criteria for common cements. Turkish Standards Institution, Ankara, Turkey.
- Zhang R, Cheng X, Hou P, Ye Z (2015). Influences of nano-TiO₂ on the properties of cement-based materials: Hydration and drying shrinkage. *Construction and Building Materials*, 81, 35–41.
- Zhang B, Tana H, Shena W, Xua G, Maa B, Jia X (2018). Nano-silica and silica fume modified cement mortar used as surface protection material to enhance the impermeability. *Cement and Concrete Composites*, 92, 7–17.